EFFICIENT CALCULATION OF NUCLEAR WAVEFUNCTIONS THROUGH COUPLING OF PROTON AND NEUTRON WAVEFUNCTIONS

A Thesis

Presented to the

Faculty of

San Diego State University

In Partial Fulfillment

of the Requirements for the Degree

Master of Science

in

Physics

---

by

Oliver Gorton

Spring 2018

SAN DIEGO STATE UNIVERSITY

The Undersigned Faculty Committee Approves the

Thesis of Oliver Gorton:

Efficient Calculation of Nuclear Wavefunctions

Through Coupling of Proton

and Neutron Wavefunctions

Calvin Johnson, Chair
Department of Physics

Kenneth Nollett
Department of Physics

Kate Rubin
Department of Astronomy

Approval Date

DEDICATION

Dedicated to Grandpa David Basta.

ABSTRACT OF THE THESIS

Efficient Calculation of Nuclear Wavefunctions
Through Coupling of Proton
and Neutron Wavefunctions
by
Oliver Gorton
Master of Science in Physics
San Diego State University, 2018

This thesis describes a nuclear shell model code which allows for a significant reduction in computer resource usage while retaining accuracy of results as compared to numerically exact solutions. I begin with an introduction to configuration interaction nuclear physics and shell model calculations. I then motivate the need for a proton-neutron decomposition of the Hamiltonian and present evidence for the viability of such a decomposition to reduce the size of the model space through three different studies. The first is a series of calculations of proton-neutron entanglement entropy, a relatively novel approach in shell model calculations. Entanglement entropy measures the distribution of singular value decomposition eigenvalues, and thus the viability of truncation of a model space. These calculations involve studying the strength and origin of the isospin dependence of the proton-neutron entanglement entropy. The second is a toy model that attempts to reproduce the entanglement entropy properties seen in realistic nuclear calculations. The third is a strength function decomposition of exact wavefunctions in an explicit proton-neutron formalism. Finally, I discuss a code to calculate nuclear wave-functions by a coupling of proton and neutron wave-functions which are calculated beforehand by an existing interacting shell model code. Results and convergence properties of this code are provided and discussed.

TABLE OF CONTENTS

PAGE

ABSTRACT v

LIST OF TABLES viii

LIST OF FIGURES ix

ACKNOWLEDGMENTS xi

CHAPTER

1 BACKGROUND 1

Introduction 1

Mathematical Background 2

Configuration Interaction Models 4

Second Quantization 5

Effective Interactions and Shell Models 7

BIGSTICK 8

Synopsis 9

2 PURPOSE 10

Statement of the problem 10

Theoretical Motivation 11

Entanglement Entropy 12

Particle-Hole Conjugates 15

Excited States and Thermalization 17

Entropy and Isospin 17

Dialing the Strength of the Proton-Neutron Interaction 18

Proton-Neutron Decomposition 20

3 PROTON NEUTRON COUPLING 26

Modified Nuclear Interactions 26

Toy Model 27

4 PNISM 36

The Hamiltonian 36

The Basis 37
Coupling 38
Matrix elements 40
One-body density matrices 41
5 COMPUTATION 44
Overview of PNISM 44
Reading in Density Matrices 45
Coupled Proton-Neutron Basis 46
Symmetries 47
Numerical methods 47
Challenges and speedups 48
6 RESULTS 50
Ground State Convergence 50
Excitation Spectra 50
Transition Strengths 50
Capstone Calculations 50
7 CONCLUSION 55
Future Improvements 55
Effective Single Particle Interactions 55
Order of Operations 55
REFERENCES 57
APPENDICES
A Supplementary Notes 59
Vector Coupling Coefficients 60
3-j Symbol 60
6-j Symbols and 9-j Symbols 60
Singular Value Decomposition 60
Lanczos Method 61
Variational Principle 61
B Sample Density Matrix Files 63
C Additional Figures 68

LIST OF TABLES

Table 1. Example target nuclei: Cs133 2

Table 2. Storage space required for nuclei in the sd and pf shell model space with the M-scheme basis in BIGSTICK[1,6] 8

Table 3. sd-shell single particle orbits 16

Table 4. Table of particle-hole conjugate nuclei in the sd-shell 16

LIST OF FIGURES

Figure 1. PN Entanglement Entropy in Particle Hole Conjugate Nuclei 18
Figure 2. PN Entanglement Entropy in Particle Hole Conjugate Nuclei (Traceless) 19
Figure 3. S vs Excitation Level: Ne 20
Figure 4. S vs Tz: SD Shell 21
Figure 5. S vs Tz: SD Shell, Traceless 22
Figure 6. Entanglement Entropy: Ne 23
Figure 7. Proton-Neutron Decomposition: Na and PH-Conjugates 25
Figure 8. Traceless interaction: Ne 27
Figure 9. Attractive Quadrapole-Quadrapole Interaction: Ne and Conjugates 28
Figure 10. Attractive Quadrapole-Quadrapole Interaction: Ti and Conjugates 29
Figure 11. Attractive pairing interaction: Ne and PH-Conjugates 30
Figure 12. Toy Model: Ground State Proton-Neutron Entanglement Entropy as a function of the TBME Scaling Factor ($lambda$). 32
Figure 13. Toy Model: Perturbative variance of the subspaces..... 33
Figure 14. Toymodel: non-separable one-body terms. 34
Figure 15. Toymodel: non-separable two-body terms. 35
Figure 16. 22Na 51
Figure 17. 28Na 51
Figure 18. 24Mg..... 52
Figure 19. 28Mg..... 52
Figure 20. Ni56 Ground State Convergence 53
Figure 21. Ni56 Excitation Spectra..... 53
Figure 22. Ni60 Ground State Convergence 54
Figure 23. Ni60 Excitation Spectra..... 54
Figure 24. S vs Excitation Level: Mg 69
Figure 25. S vs Excitation Level: Ne..... 70
Figure 26. S vs Excitation Level: Ne..... 70
Figure 27. S vs Tz: SD-PF Shell 71

Figure 28. S vs Tz: PF Shell 71
Figure 29. S vs Coupling: Mg 72
Figure 30. S vs Coupling: Cr 72
Figure 31. S vs Coupling (Traceless): Na 73
Figure 32. S vs Coupling (Traceless): Cr 73
Figure 33. S vs Coupling (QQ): Na 74
Figure 34. S vs Coupling (QQ): Mg 74
Figure 35. S vs Coupling (QQ): V 75
Figure 36. S vs Coupling (QQ): Cr 75
Figure 37. Proton-Neutron Decomposition: Ne and PH-Conjugates 76
Figure 38. Proton-Neutron Decomposition: Mg and PH-Conjugates 76
Figure 39. Proton-Neutron Decomposition: Al and PH-Conjugates 77

ACKNOWLEDGMENTS

Thank you goes here.

CHAPTER 1

BACKGROUND

INTRODUCTION

Nuclear physics is the study of the structure and properties of atomic nuclei, which make up most of the known matter in the universe. The goal of nuclear theory to make predictions about the interactions of nuclei with external fields, in order to answer questions about experimental outcomes and thereby deeper and ongoing questions in physics about the fundamental symmetries of nature.

Some of the more important and open questions in physics, such as those related to the matter and antimatter symmetry violation, the source and origin of dark matter in the universe, and neutrinoless double beta decay, rely on accurate and detailed quantum models of nuclei. In order to understand observations obtained from experiments, we need to be able to compute the expectation values of operators with accurate wavefunctions computed from detailed Hamiltonians. This is an extremely diffucult task on two interrelated fronts. The first is the theoretical front where we face the problem of reproducing global and microscopic properties of the nucleus. The second is the of diagonalizing (solving) the model and computing observables. In any model, the cost of solving a problem must be weighed against the accuracy and completeness of the results.

As with any N-body problem, the nuclear many body problem can very quickly become computationally intractable, even for relatively light nuclei. Thus advanced computational methods and high performance computing are necessary to accurately carry out nuclear matrix element calculations for large nuclei. The goal of this project is to reduce the computational resources necessary for the calculation of larger nuclei necessary for modern experimental physics. As a particular example, calculations of nuclear anapole moments for nuclei including ^{133}Cs and ^{205}Tl rely on accurate ground state wavefunctions and one- and two-body density matrix elements. However, ^{133}Cs in the configuration interaction shell model representation has a basis dimension of over one-hundred million and requires nearly

800GB of memory to store just the non-zero matrix elements of the Hamiltonian. While these are not impossibly large computational problems, clearly there is a need for an accurate approximation scheme.

Nuclide	Val. P	Val. N	Basis dim.	Storage (GB)
^{133}Cs	5	28	1.98×10^8	796.2
^{105}Cs	5	0	7451	0.6×10^{-2}
^{128}Sn	0	28	1504	0.8×10^{-3}

Table 1. Example target nuclei: Cs133

Our approach is to work in a proton-neutron formalism and to solve separately the neutron-neutron interaction and the proton-proton interaction. These results then coupled together to obtain the full wavefunction. ^{105}Cs and ^{128}Sn are non-physical nuclei; they are wavefunctions calculated containing only valence protons and only valence neutrons, respectively. These wavefunctions are then used to create a basis of coupled proton-neutron wavefunctions. This basis is truncated and used to calculate the matrix elements of the ^{133}Cs Hamiltonian. In this way we hope to obtain accurate approximate nuclear wavefunctions. To give as estimate of the reduction in the size of the problem, we could consider truncating the coupled proton-neutron basis to 750 states, down from the maximum of 7451 in the case of the proton space. This would result in a total Hamiltonian matrix dimension of 5.6×10^5, a three order of magnitude reduction. (Note that Sn128 with 28 valence neutrons has a smaller dimension thatn Cs105 with five valence protons. This is because the symmetries of the occupation representation in a shell model space allow us to treat 28 valence neutrons as four valence neutron holes.)

MATHEMATICAL BACKGROUND

In this and the following section I give a brief introduction to the mathematical underpinning of the nuclear many body problem. I assume an understanding of undergraduate quantum mechanics.

Since the nucleus is a quantum mechanical object, nuclear physics is essentially a quantum many-body problem. Much of nuclear physics can be explained by the (non-relativistic) N-body Schrödinger equation:

$$\hat{H}\Psi(\vec{r}_1, \vec{r}_2, \vec{r}_3, ..., \vec{r}_N) = E\Psi(\vec{r}_1, \vec{r}_2, \vec{r}_3, ..., \vec{r}_N). \quad (1)$$

Here, $\hat{H}$ is the Hamiltonian which includes kinetic energy and potential energy terms for each particle. The potential energy contains the nuclear interaction and/or other relevant interactions like the Coulomb force.[1] Ψ is our wave-function, a function of the position of every particle in the system. If we could solve the Schrödinger equation for any system, the task of the theoretical nuclear physicist would be complete. However, in general, there is no analytic solution to (1) except for in a very small number of cases involving a great deal of symmetry and a small number of particles. In any practical situation where calculations of realistic nuclear structure are required, numerical methods are necessary.

Towards this end, let's review the matrix formulation of quantum mechanics. Let us start with an eigenvalue equation of the form

$$\hat{H}|\Psi\rangle = E|\Psi\rangle. \tag{2}$$

$\hat{H}$ is a linear operator on a Hilbert space $\mathcal{H}$ and $|\Psi\rangle$ is a state vector which is a member of the Hilbert space. By the definition a basis of the Hilbert space, any basis $\{|\alpha\rangle\}$ must satisfy the completeness relation

$$1 = \sum_{\alpha} |\alpha\rangle\langle\alpha|, \tag{3}$$

thus any state vector $|\Psi\rangle$ can be expressed as the following, where $\Psi_\alpha \equiv \langle\alpha||\Psi\rangle$

$$|\Psi\rangle = \sum_{\alpha} \Psi_\alpha |\alpha\rangle. \tag{4}$$

For this to be meaningful we will eventually need to choose a particular basis to work in. Starting again from (2) and substituting this representation of our eigenstate,

$$H \sum_{\alpha} \Psi_\alpha |\alpha\rangle = E \sum_{\alpha} \Psi_\alpha |\alpha\rangle \tag{5}$$

and projecting onto a dual basis state $\langle\beta|$

$$\begin{aligned} \langle\beta|H \sum_{\alpha} \Psi_\alpha |\alpha\rangle &= \langle\beta|E \sum_{\alpha} \Psi_\alpha |\alpha\rangle \\ \sum_{\alpha} \langle\beta|H|\alpha\rangle \Psi_\alpha &= \sum_{\alpha} \langle\beta||\alpha\rangle E \Psi_\alpha \\ \sum_{\alpha} H_{\beta\alpha} \Psi_\alpha &= E \Psi_\beta. \end{aligned} \tag{6}$$

Where the matrix elements of $\hat{H}$ are defined to be

$$H_{\beta\alpha} \equiv \langle\beta|\hat{H}|\alpha\rangle. \tag{7}$$

Now that we have converted the Schrodinger equation into a matrix eigenvalue problem, it becomes theoretically straightforward to obtain important results such as the energy spectra of nuclei, and transition probabilities; simply diagonalize the Hamiltonian matrix to obtain the energy spectra (eigenvalues), wavefunctions (eigenvectors) and density matrices for computing observables.

Complications include the fact there is really no way to write down a simple analytic Hamiltonian for the nuclear force like there is for classical forces such as gravity or the coulomb force. The nuclear interaction is mediated by the gauge bosons of the strong and weak nuclear force (gluons, Z and W bosons). Furthermore, even once a Hamiltonian is obtained, solving for its eigenvalues can be a non-trivial computational problem - when the dimensions of the space can be as high as a few billion. There are a number of popular computational methods for solving the many-body Hamiltonian, of which the configuration interaction method is an example. This is further discussed below.

The Hamiltonian used in this non-relativistic approximation is most rigorously (from the theoretical point of view) derived from what is known as chiral perturbation theory, which comes from quantum chromodynamics.[2] Today, interactions are found from variational methods by fitting to experimental data. (i.e. the NNDC.[3]) We use phenomenological interactions.

CONFIGURATION INTERACTION MODELS

The defining feature of the configuration interaction model is to write the many-body basis states $\{|\alpha\rangle\}$ used above in terms of anti-symmetrized products of single-particle solutions to a single-particle Hamiltonian. Let's explore what this means.

Because our wave-functions Ψ live in a vector space (more precisely, in a Hilbert space) we can always rewrite Ψ in another basis of our choosing.

$$\Psi(\vec{r}_1, \vec{r}_2, \vec{r}_3, ..., \vec{r}_N) = \sum_\alpha c_\alpha \Phi_\alpha(\vec{r}_1, \vec{r}_2, \vec{r}_3, ..., \vec{r}_N) \tag{8}$$

This is an N-body wavefunction with N sets of coordinates, one for each particle. The CI method is to choose our Φ to be a product of single-particle wave functions,

$$\{\phi_a\},\ a = 1, ..., d, \tag{9}$$

where d is the number of single-particle states. These single-particle wavefunctions are chosen to be some convenient basis that will span the Hilbert space of interest. However, they

need not be manifestly related to a physically meaningful Hamiltonian. This is the case in phenomenological interactions, which are discussed later on. Other combinations of single-particle states are possible, of course, but they don't have trivial normalization. The normalization integral of a product wavefunction is simply the product of the integrals of each factor. However, rather than a direct product of single- particle wavefunctions, we instead choose the more complicated rule:

$$\Phi(\vec{r}_1, \vec{r}_2, \vec{r}_3, ..., \vec{r}_N) = \frac{1}{\sqrt{N}} \sum_{i_1, i_2, ..., i_N}^{N} \epsilon_{i_1, i_2, ..., i_N} \phi_1(\vec{r}_{i_1}) \phi_2(\vec{r}_{i_2}) \phi_3(\vec{r}_{i_3}) ... \phi_d(\vec{r}_{i_N}), \tag{10}$$

viz. the determinant of the matrix defined by $[\phi_a(i_b)]$ with a normalization factor, with index a labeling the single-particle state and index i_b labeling the particle number. This is a product of single-particle wavefunctions with the additional property that it is anti-symmetric: exchanging any two i_b (any two columns) would change the sign of the overall wavefunction; a general property of determinants. This is encoded in the Levi-Civita symbol $\epsilon_{i_1, i_2, ..., i_N}$.[4] Since nuclei are composed of protons and neutrons, which are spin-1/2 particles (fermions), we must have antisymmetric wave-functions. By defining our many-body wave-functions to be determinants of single-particle wavefunctions we have enforced antisymmetric many-body states. These specially constructed states are known as Slater determinants.

SECOND QUANTIZATION

Occupation representation is an additional formalism that is used to further compactify our representation of wavefunctions. Although this topic is very broad and goes very deep, here I will only state the relevant results of this so-called second quantization formalism. This formalism begins by giving up coordinate representation, or other quantum number representation of wavefunctions, in favor of occupation number. Many-body basis states are no longer represented as the product of coordinate functions of single particle states. Instead, a basis of single-particle states is chosen, perhaps the same set $\{\phi_a\}$ as above, and the many-body states are represented in the abstract as

$$\Psi(\vec{r}_1, \vec{r}_2, \vec{r}_3, ..., \vec{r}_N) \rightarrow \Psi\{n_\phi\} = |n_1, n_2 ... n_d\rangle, \tag{11}$$

where n_a is the number of particles in the state ϕ_a. Without any additional structure, this representation lacks anti-symmetry; this is restored by representing the state $|n_1, n_2 ... n_d\rangle$ as the action of a series of operators on the vacuum state $|0, 0 ... 0\rangle$. The operator which turns

$|0,0...0\rangle$ into $|1,0...0\rangle$ is called the creation operator, and the operator which turns $|1,0...0\rangle$ into $|0,0...0\rangle$ is called the anhiliation operator. For fermions, these two generalized ladder operators are defined implicitly through their anti-commutation relations:[5]

$$\begin{aligned} \{\hat{a}_i, \hat{a}_j^\dagger\} &\equiv \hat{a}_i\hat{a}_j^\dagger + \hat{a}_j^\dagger\hat{a}_i = \delta_{ij} \\ \{\hat{a}_j, \hat{a}_j\} &= \{\hat{a}_i^\dagger, \hat{a}_j^\dagger\} = 0 \end{aligned} \tag{12}$$

These anti-commutation relations encode the properties of systems of fermions: two fermions cannot occupy the same state, $(\hat{a}_i^\dagger)^2 = 0$, and therefore the maximum occupancy of a state ϕ_i is one. Thus,

$$\begin{aligned} &\hat{a}_1^\dagger|1,0,...,0\rangle = 0, \\ &\hat{a}_1^\dagger|0,0,...,0\rangle = |1,0,...,0\rangle, \\ &\hat{a}_1|1,0,...,0\rangle = |0,0,...,0\rangle, \\ &\hat{a}_1|0,0,...,0\rangle = 0, \end{aligned} \tag{13}$$

and so on for any state $|n_1, n_2...n_d\rangle$. With this mathematically equivalent structure, we can replace our slater determinants (10) with occupation representations using second quantization operators. Any many body state can now be written

$$\Phi = |n_1, n_2...n_d\rangle = (\hat{a}_1^\dagger)^{n_1}...(\hat{a}_d^\dagger)^{n_d}|0,...,0\rangle. \tag{14}$$

Since each state's occupation n_i is contrained to a 0 or a 1, many body states can be represented by bit strings. For example,[6]

$$\hat{a}_1^\dagger\hat{a}_4^\dagger\hat{a}_5^\dagger\hat{a}_7^\dagger|\rangle \rightarrow 1001101, \tag{15}$$

where here we are dealing with a four-body wavefunction in a basis with at least seven single-particle states, and where I have used $|\rangle$ here in place of $|0,...,0\rangle$ for brevity. This makes computer storage of wavefunctions trivial.

It can be shown that one-body operators can be expressed in the second quantization formalism as:[7]

$$\hat{O} = \sum_{ij}\langle i|O|j\rangle\hat{a}_i^\dagger\hat{a}_j, \tag{16}$$

where the sum is over all single-particle states. Similarly, two-body operators can be expressed:[7]

$$\hat{O} = \frac{1}{4}\sum_{ijkl}\langle ij|O|kl\rangle\hat{a}_i^\dagger\hat{a}_j^\dagger\hat{a}_k\hat{a}_l. \tag{17}$$

The factor of one-fourth comes from the fact that the sum is over all single- particle states and would otherwise overcount the number of (pairwise) interactions. The Hamiltonian may be rewritten using these representations:

$$\hat{H} = \sum_{i,j} \hat{a}_i^\dagger \langle i|T|j\rangle \hat{a}_j + \frac{1}{4} \sum_{i,j,k,l} \hat{a}_i^\dagger \hat{a}_j^\dagger \langle ij|V|kl\rangle \hat{a}_l \hat{a}_k, \tag{18}$$

where the first term represents the one-body interactions such as kinetic energy or the Coulomb interaction with an external field, and the second term represents two-body interactions (forces between interacting particles) and contains the nuclear force. This formalism is key to the way this model is translated into powerful computer codes which can be used for a number of different calculations.

EFFECTIVE INTERACTIONS AND SHELL MODELS

The basis of single particle states that are used in shell model methods are seldom derived from fully realistic calculations. A truly realistic model of the nucleus would necessarily involve the description of the exchange of mesons.[8] Instead, single particle states are taken to be solutions to (non-field theory) quantum potentials. Some variation of a mean-field approximation is used to approximate the nuclear interaction. This could a harmonic oscillator, or the more sophisticated Woods-Saxon potential.[7]

To reach larger nuclei in configuration interaction methods, it's necessary to employ model interactions that leave out part of the configuration space. It's possible to compute an effective interaction to account for this missing part. By enforcing that the effective interaction acting on the model wavefunction reproduces the same results as the full interaction on the full wavefunction, one can expand the effective interaction into a series of the form[9]

$$V^{eff} = V + V\frac{\hat{Q}}{E - H_0}V + ... \tag{19}$$

where $\hat{Q}$ is a projection operator onto the part of the full Hilbert space that was left out of the model. In shell model codes, the vacuum state is redefined to be an inert core of nucleons, and the model space to be a limited space of particle-hole excitations near a Fermi surface.[9] To reach nuclides in the sd-shell, for example, one uses an inert O16 core with 8 non-interacting protons and 8 non-interacting neutrons, the overall effect of which is to add an effective energy to a single-particle model.[9]

BIGSTICK

We use a configuration interaction code called BIGSTICK.[1,6] BIGSTICK uses the so-called M-scheme basis choice, meaning the J_z quantum number m is held fixed. This works because it assumes the the Hamiltonian is rotationally invariant - a valid assumption for most applications. BIGSTICK is unique because of its Hamiltonian factorization algorithm. By factorizing both the basis and the interaction the amount of memory necessary can be drastically reduced, up to an order of magnitude. The factorized basis and interaction are used to reconstruct only the pieces of the Hamiltonian that are needed, and only when they are needed.

The primary functionality of BIGSTICK is to calculate the energy spectra and angular momentum of a finite number of low-lying energy states. However it is a large code with many capabilities including calculating transition strength functions and decompositions of wave-functions into different bases.[1,6]

Despite the fact that the interaction files used to build the basis for the space are semi-empirical, BIGSTICK and codes like it are still 'numerically exact', that is, they don't use any numerical approximations once the Hamiltonian is built. This means that BIGSTICK can still be extremely computationally expensive to run for large nuclei. Fortunately this is curbed by the algorithm mentioned above, and by other methods such as basis truncation and inert-core models. Below is a table of the storage space (RAM) required to store the nonzero matrix elements for various nuclei in different phenomenological model spaces.

Nuclide	Space	Basis dim.	Storage (GB)
^{28}Si	sd	9.4×10^4	0.2
^{52}Fe	pf	1.1×10^8	720
^{56}Ni	pf	1.1×10^9	9600

Table 2. Storage space required for nuclei in the sd and pf shell model space with the M-scheme basis in BIGSTICK[1,6]

The Hamiltonian used in this non-relativistic approximation is most rigorously (from the theoretical point of view) derived from what is known as Chiral perturbation theory, which comes from quantum chromodynamics.[2] Today, interactions are found from variational methods by fitting to experimental data. (i.e. the NNDC.[3]) Despite this, results have fairly low

errors of around a few hundred KeV relative to experiment(low-lying states tend to be a few MeV in magnitude).

SYNOPSIS

The configuration interaction method of nuclear physics is useful because it allows us to reframe the quantum many-body problem for nuclei in terms of known one-body solutions which can then be combined into an eigenvalue problem for the many-body system. Furthermore the formalism has many nice properties built into it that make computations easier. If one begins with normalized single-particle states, then constructing an orthonormal many-body wave-function is trivial using product wave-functions. Using Slater determinants of being anti-symmetric and so respects the Pauli exclusion principle. Slater determinant wave-functions also easily transfer to the ocupation representation (quantization of quantum operators). The Hamiltonian can be factorized for reduction in memory usage. And the effective model space can be reduced with inert shells.

CHAPTER 2

PURPOSE

STATEMENT OF THE PROBLEM

Because of the intense computational cost of solving nuclear structure problems, and the limited computer resources available, it is necessary to pursue approximation methods in order to obtain accurate enough solutions in short enough periods of time. The purpose of this thesis is to investigate the viability of a particular factorization scheme wherein the basis used by an existing interacting shell model code is decomposed into pure-proton and pure-neutron wavefunctions, plus a term which isolates the proton-neutron interaction.

A similar study has been carried out before.[10–12] The main results of those papers relevant here are that the shell model basis states are approximated by retaining only a few number of factors in a sum over products of pure proton and pure neutron wavefunctions. Ground states in *sd* and *pf* shell as well as low-lying states converge to full diagonalization results exponentially as the number of factors retained is increased. The authors examine mostly $N = Z$ nuclei but predict that the method would be viable for other nuclei as well. The authors also provide no explaination for the cause of the exponential convergence.

This thesis begins with a related analysis of SVD values in a proton-neutron basis, but utilizes proton-neutron entanglement entropy to examine the strength of the proton-neutron coupling. A hypothesis is tested which predicts that this proton-neutron coupling scheme will be even more effective for nuclei where the number of neutrons is much larger than the number of protons, i.e. for large isospin. This thesis spends significant time on the investigation of the the properties of proton-neutron entanglement entropy, paying special attention to its correlation with of this scheme in $N > Z$ nuclei. Additionally, while the SVD papers were restricted to relatively low dimensional problems, we apply this method to very large problems where full diagonalization schemes are not viable.

This thesis begins by generating evidence that the creation of approximate wavefunctions through coupling of proton and neutron wavefunctions may be a valueble

method. By decomposing existing wavefunctions from BIGSTICK, we conduct two related studies: first, a singular value decomposition of BIGSTICK wavefunctions, from which we extract the proton-neutron entanglement entropy. Second, we decomposed BIGSTICK wavefunctions into pure-proton and pure-neutron components by projecting the existing wavefunctions onto the appropriate operators.

THEORETICAL MOTIVATION

We can always expand a wavefuntion into any basis. Suppose we have some initial representation of our wavefunction,

$$|\Psi\rangle = \sum_{i_p,j_p} \Psi_{i_p,j_n} |i_p\rangle |j_n\rangle, \tag{20}$$

where the uncoupled basis states are Slater determinants

$$\begin{aligned} |i_p\rangle, i_p = 1, d_p, \\ |j_n\rangle, j_p = 1, d_n \end{aligned} \tag{21}$$

We choose to decompose our wavefunction $|\Psi\rangle$ into pure proton $|\pi_a\rangle$ and pure neutron $|\nu_b\rangle$ wavefunctions which are related to the old basis states by some unitary transformation. We can always find such a unitary transformation between the basis state $|i_p\rangle$ and $|\pi_a\rangle$,

$$|\pi_a\rangle = \sum_{i_p} U^{\pi}_{a i_p} |i_p\rangle, \tag{22}$$

and similarly for $|j_n\rangle$ and $|\nu_b\rangle$. Thus we can find

$$|\Psi\rangle = \sum_{a,b} \tilde{\Psi}_{ab} |\pi_a\rangle |\nu_b\rangle, \tag{23}$$

where a enumerates proton single-particle states and b enumerates neutron single-particle states. If the sum is taken over all states, (23) is equivalent to (20). The goal, however, is to find a basis in which the sum (23) can be truncated, thus reducing the size of the problem.

$$|\Psi\rangle = \sum_{a,b=1}^{N} \tilde{\Psi}_{ab} |\pi_a\rangle |\nu_b\rangle, \quad N << \min(d_p, d_n). \tag{24}$$

In order for the truncated sum to be useful, the terms we exclude must be small compared to the overall wavefunction. It's not obvious whether or not such a basis exists, or how to find it if one did exist. If we knew of a basis where the wavefunctions of interest had simple (easily

truncated) representations, then it would be ideal to compute the matrix elements of our Hamiltonian in that truncated basis. The next section explains the method we will use to generate evidence for the existence of a basis where our nuclear wavefunctions can be significantly truncated.

ENTANGLEMENT ENTROPY

If we have some normalized representation of a wavefunction,

$$|\Psi\rangle = \sum_{\alpha} c_{\alpha} |\Phi_{\alpha}\rangle, \tag{25}$$

then the sum of the weights $|c_{\alpha}|^2$ is unity:

$$1 = \sum_{\alpha} |c_{\alpha}|^2. \tag{26}$$

The distribution of the weights $|c_i|^2$ tells us how much the sum (25) can be truncated in the basis $|\Phi_i\rangle$. In a basis of coupled single particle states as in (24) and (23), the coefficients form a nonsymmetric matrix. However, we can use a singular value decomposition (see Appendix (A.4)) to examine quantities which are invariant under a unitary transformation such as equation (22). The distribution of singular value decomposition (SVD) eigenvalues will tell us how much we can truncate the expansion (24).

A singular value decomposition is a factorization of any matrix A into the following form:

$$A = UDV^{\dagger}, \tag{27}$$

where U and V are unitary matrices and D is a diagonal matrix. The diagonal elements of D are the SVD eigensvalues. See appendix A.4 for more information about singular value decompositions. The matrices don't have to be square. Notice that if we compute $AA^{\dagger}$ we find:

$$\begin{aligned} AA^{\dagger} &= UDV^{\dagger}(UDV^{\dagger})^{\dagger} \\ &= UDV^{\dagger}VD^{\dagger}U^{\dagger} \\ &= UDD^{\dagger}U^{\dagger}, \end{aligned} \tag{28}$$

where now $D^{\dagger}D = D^2$ is diagonal, square, and positive definite. SVD eigenvalues can thus be obtained and diagonalizing $AA^{\dagger}$. Equation (28) represents a unitary transformation of a

matrix, therefore the SVD eigenvalues are invariant. This means that the SVD eigensvalues of the coefficients in the expansion (24) can found by diagonalizing the matrix

$$(AA^{\dagger})_{a'a} = \sum_{b} \tilde{\Psi}_{a'b}\tilde{\Psi}^{*}_{ba}, \tag{29}$$

or by diagonalizing the matrix

$$(AA^{\dagger})_{a'a} = \sum_{b} \Psi_{a'b}\Psi^{*}_{ba}, \tag{30}$$

from the coefficients in equation (20) which we already have. Previously is has been shown that ground state SVD eigenvalues fall off rapidly in a basis of coupled proton-neutron states.[10] This suggests that such a truncation scheme exists and yields accurate approximations to shell model ground states and low-lying states.[11] We will show in this chapter is that this method is even more effective in nuclei with higher isospin. To show this, we will use a compact metric for analyzing the distribution of SVD eigenvalues, the proton-neutron entanglement entropy. Next I will explain what the proton-neutron entanglement entropy is and where it comes from.

Equation (30) is simply the reduced density matrix of the eigenstate $|\Psi\rangle$ in the choice of basis given in (20). The *density operator* of a pure state Ψ is defined as

$$\rho = |\Psi\rangle\langle\Psi|. \tag{31}$$

Given the choice of basis shown in equation (20), we can compute the following density matrix:

$$\rho_{a'b'ab} = \Psi_{a'b'}\Psi^{*}_{ba}. \tag{32}$$

If the Hilbert space is bipartite $\mathcal{H}^{\pi\nu} = \mathcal{H}^{\pi} \otimes \mathcal{H}^{\nu}$ then we can define the reduced density operator of a particular subspace $\mathcal{H}_p$ to be

$$\rho^{\pi} = tr_{\nu}\rho^{\pi\nu}, \tag{33}$$

where $\rho^{\pi\nu}$ is a density operator in the space $\mathcal{H}^{\pi\nu}$. The reduced density matrix ρ^{π} in our choice of basis is computed from (32):

$$\begin{aligned} \rho^{\pi}_{a'a} &= tr_{\nu}(\rho_{a'b'ab}) \\ &= \sum_{b} \Psi_{a'b}\Psi^{*}_{ba} \\ &= (AA^{\dagger})_{a'a}. \end{aligned} \tag{34}$$

In the SVD papers cited earlier, this density matrix was only used to compute the SVD eigenvalues. Here, we are going to take advantage of the information of mixing that is contained within the density matrix: the entanglement entropy.

The *von Neumann entropy* is defined in terms of the generalized density operator (quantum state ρ) by

$$S(\rho) \equiv -tr(\rho\, ln\rho). \tag{35}$$

The *entanglement entropy* of a state in a bipartite system $\mathcal{H}^{\pi\nu} = \mathcal{H}^{\pi} \otimes \mathcal{H}^{\nu}$ is the von Neumann entropy of a reduced density matrix:

$$S(\rho^{\pi}) = -tr(\rho^{\pi} ln \rho^{\pi}). \tag{36}$$

In our case, the (proton-neutron) entanglement entropy measures the number of quantum bits shared between the proton and neutron spaces. It is also a measure of the distribution of the SVD eigenvalues. It can be shown that $S(\rho^{\pi}) = S(\rho^{\nu})$, which is related to the invariance of SVD eigenvalues. We therefore simply refer to $S_{pn} \equiv S(\rho^{\pi}) = S(\rho^{\nu})$ as the proton-neutron entanglement entropy. We first diagonalize the density matrix ρ_{π} and compute S_{pn} using the eigenvalues $\{\gamma_i^2\}$ of ρ_{π} so that

$$S_{pn} = -\sum_i \gamma_i^2\, ln(\gamma_i^2), \tag{37}$$

where γ_i are also the SVD eigenvalues of $\tilde{\Psi_{ab}}$ and $\Psi_{i_p j_n}$. The proton-neutron entanglement entropy for a given state $|\Psi\rangle$, is a measure of the entanglement of the two partitions of the Hilbert space and it indicates the degree to which an expansion

$$|\Psi\rangle = \sum_i \gamma_i |\tilde{\pi}_i\rangle |\tilde{\nu}_i\rangle \tag{38}$$

can be truncated. If the entanglement entropy is zero, for example, then (38) contains only one term. A maximal value of S_{pn} would indicate that each term in the expansion is equally weighted; then we would have

$$S_{max} = ln(N_p). \tag{39}$$

Then a lower proton- neutron entanglement entropy corresponds to a system in which we can get a more accurate representation of our state $|\Psi\rangle$ with fewer states in (38). Where the proton-neutron entanglement entropy has an advantage over the raw distribution of SVD values is the ability to compare different states with a single number. In particular, if the

proton-neutron entanglement entropy is smaller in nuclei where isopin is large, then we can expect such a truncation scheme to be more effective for large isospin nuclei. This is good news for the calculation of large nuclei with a large excess of neutrons. Cesium 133 has 40% more neutrons than protons, for example. However, and this is critical, we are not guarenteed to find the optimal basis $\{|\tilde{\pi}_i\rangle|\tilde{\nu}_i\rangle\}$, we are only generating evidence that one exists.

We will compute the proton-neutron entanglement entropy and demonstrate that it is significantly lower for $N > Z$ nuclei than for $N = Z$ nuclei, even for nuclei with the same model space dimensions. First I will justify the use of low proton-neutron entanglement entropy as an indicator of the existence of a basis which can yield accurate truncated representations.

Particle-Hole Conjugates

Note that the proton-neutron entanglement entropy depends on the dimension of the model space. In order for the proton-neutron entanglement entropy to be useful in comparing $N > Z$ nuclei to $N = Z$ nuclei, we need to compare sets of nuclei with equal or similar dimensionality. That way, two nuclei with equal dimensions will differ in proton-neutron entanglement entropy only because of some phenomenon rooted in the properties of the interaction. To do this, we choose to compare sets of nuclei which are particle-hole conjugates. Recall that in the interacting shell model, we redefine the vacuum state in terms of some inert core of noninteracting nucleons. The single particle model space is then taken to be a system of interacting particles and particle holes. A particle hole is a gap in an otherwise filled shell.

In an interacting particle-hole shell model space, the number of valence particles is restricted to some maximum value. Within a model space, a filled particle state is dimensionally equivalent to a particle hole. Two nuclei which are particle-hole conjugate have the same number of neutrons holes or particles and the same number of proton holes or particles. For example, ^{18}F in the sd-shell with an inert ^{16}O core has 8 inert protons and 8 inert neutrons, with one valence proton and one valence neutron, both of which are in the $0d_{3/2}$ single particle orbit. The sd-shell model space has a maximum of 12 valence particles of each type, since the space ($0d_{3/2}$, $0d_{5/2}$ and $1s_{1/2}$) has 12 unique quantum numbers in n, l, j, m. Thus ^{18}F has 12 possible states each for the proton and neutron. ^{38}K, which has 11 valence protons and 11 valence neutrons, can be represented by two particle holes in the completely

filled sd-shell model space, and thus also has 12 possible states. Table (3) contains the complete set of sd-shell model space quantum numbers.

Orbit	n	l	j	m	Degeneracy	Max fill
$0d_{3/2}$	0	2	3/2	3/2, 1/2, -1/2, -3/2	4	4
$0d_{5/2}$	0	2	5/2	5/2, 3/2, 1/2, -1/2, -3/2, -5/2	6	10
$1s_{1/2}$	1	0	1/2	1/2, -1/2	2	12

Table 3. sd-shell single particle orbits

Table (4) is a collection of nuclei for which the proton-neutron entanglement entropy of the ground state were computed. Each row in the table is a particle-hole conjugate triplet, meaning every nucleus is listed in the same row as its particle-hole conjugates

Inert Core	Nucleus	(Zval, Nval)					$d_p = d_n$
16O	^{18}F	(1,1)	^{28}F	(1,11)	^{38}K	(11,11)	12
Max 12	^{20}Ne	(2,2)	^{28}Ne	(2,10)	^{36}Ar	(10,10)	66
	^{22}Na	(3,3)	^{28}Na	(3,9)	^{34}Cl	(9, 9)	220
	^{24}Mg	(4,4)	^{28}Mg	(4,8)	^{32}S	(8, 8)	495
	^{26}Al	(5,5)	^{28}Al	(5,7)	^{30}P	(7, 7)	792
40Ca	^{42}Sc	(1,1)	^{60}Sc	(1,19)	^{78}Y	(19,19)	20
Max 20	^{44}Ti	(2,2)	^{60}Ti	(2,18)	^{76}Sr	(18,18)	190
	^{46}V	(3,3)	^{60}V	(3,17)	^{74}Rb	(17,17)	1140
	^{48}Cr	(4,4)	^{60}Cr	(4,16)	^{72}Kr	(16,16)	4845
56Ni	^{58}Cu	(1,1)	^{78}Cu	(1,21)	^{98}In	(21,21)	22
Max 22	^{60}Zn	(2,2)	^{78}Zn	(2,20)	^{96}Cd	(20,20)	231
	^{62}Ga	(3,3)	^{78}Ga	(3,19)	^{94}Ag	(19,19)	1540
	^{64}Ge	(4,4)	^{78}Ge	(4,18)	^{92}Pd	(18,18)	7315
100Sn	^{102}Sb	(1,1)	^{132}Sb	(1,31)	^{162}Ti	(31,31)	32
Max 32	^{104}Te	(2,2)	^{132}Te	(2,30)	^{160}Hg	(30,30)	496
	^{106}I	(3,3)	^{132}I	(3,29)	^{158}Au	(29,29)	4960

Table 4. Table of particle-hole conjugate nuclei in the sd-shell

Figure (1) is a collection of proton-neutron entanglement entropies for the nuclei listed in table (4). The vertical axis is the relative proton- neutron entanglement entropy and each particle-hole conjugate triplet lies in a given column and is labeled according to its representative nucleus. Each row in table (4) is plotted in its own column. For example, the

data points above "^{18}F" on the horizontal axis are ^{18}F ($N = Z$), ^{28}F ($N > Z$) and ^{38}K ($N = Z$). Each of the four frames in the figure corresponds to a different shell-model space listed in table 4).

Figure (1) demonstrates that nearly all particle-hole triplets in the four model spaces tested have the lowest proton-neutron entanglement entropy in nuclei where $N > Z$. The exceptions are the ^{18}F, ^{22}Na, and ^{26}Al triplets in the sd-shell model space and the ^{42}Sc triplet in the *pf*-shell model space. All four of these exceptions are odd-odd nuclei. Figure (2) is the same plot with a two-body interaction with monopole terms removed (traceless interaction). This type of interaction is discussed in greather detail in the next chapter so I won't go into detail here. This plot is included here to emphasize the difference between $N = Z$ nuclei, which are degenerate in entanglement entropy in traceless interactions, and $N > Z$ nuclei. With the monopole terms removed from the nuclear interaction, all $N > Z$ nuclei have significantly lower proton-neutron entanglement entropy than their particle-hole conjugte $N = Z$ pairs.

These suggest that

Excited States and Thermalization

In order for our approach to be viable, we will need the pattern exhibited in the previous sections to hold for not just the ground state, but for excited states as well. By plotting the proton-neutron entanglement entropy for many a number of the lowest energy levels, we see that $N > Z$ nuclei tend to have the lowest proton-neutron entanglement entropies only for the first few lowest eigenstates. After this, the ordering becomes apparently random. We came to the conlcusion that we are observing a kind of thermalization. As the energy of the system increases, the low entropy configurations expressed in $N > Z$ nuclei disappear.

Entropy and Isospin

So far we have demonstrated on a case by case basis that $N > Z$ nuclei tend to have lower proton-neutron entanglement entropy than their particle-hole conjugates. The next kind of plot that we examined are plots of proton-neutron entanglement entropy S versus isospin, specifically the z-component of the isospin T_z. We will use the convention that for protons $T_z = -\frac{1}{2}$ and that for neutrons $T_z = +\frac{1}{2}$. We can then compute the maximum value of T_z for a

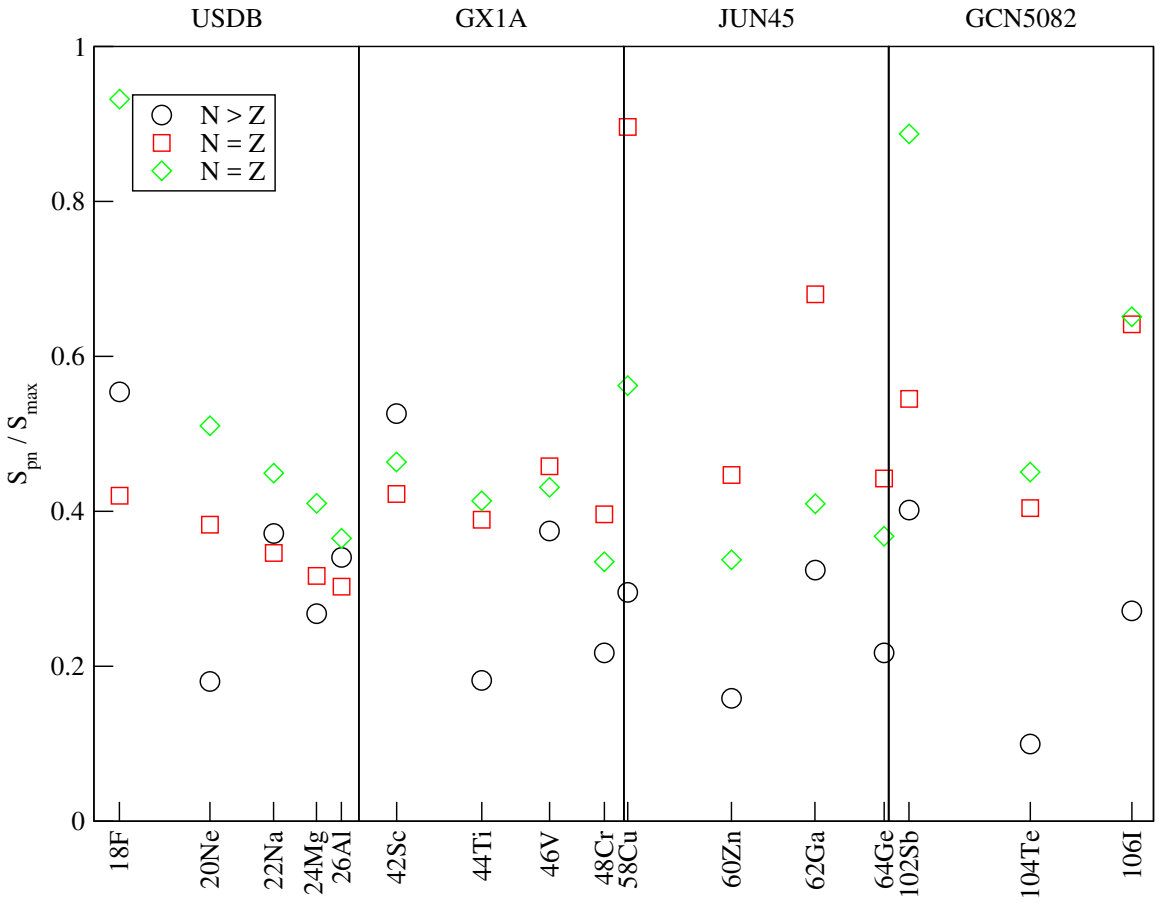

Figure 1. PN Entanglement Entropy in Particle Hole Conjugate Nuclei

given nucleus as $\frac{1}{2}(N-Z)$. As shown in figures 4 and 5, as T_z increases, the proton-neutron entanglement entropy tends to decrease. This was shown in both the sd shell and the pf shell. Additional S versus T_z plots are provided in appendix C. We also extended the analysis to the sd-pf shell model space where we examined non physical nuclei with value of T_z as high as $T_z = 14$.

Dialing the Strength of the Proton-Neutron Interaction

BIGSTICK to allows for scaling of the proton-neutron interaction term when working in the explicit proton-neutron formalism. Thus the two-body part of Hamiltonian is of the form

$$H = H_{pp} + H_{nn} + \lambda H_{pn}. \tag{40}$$

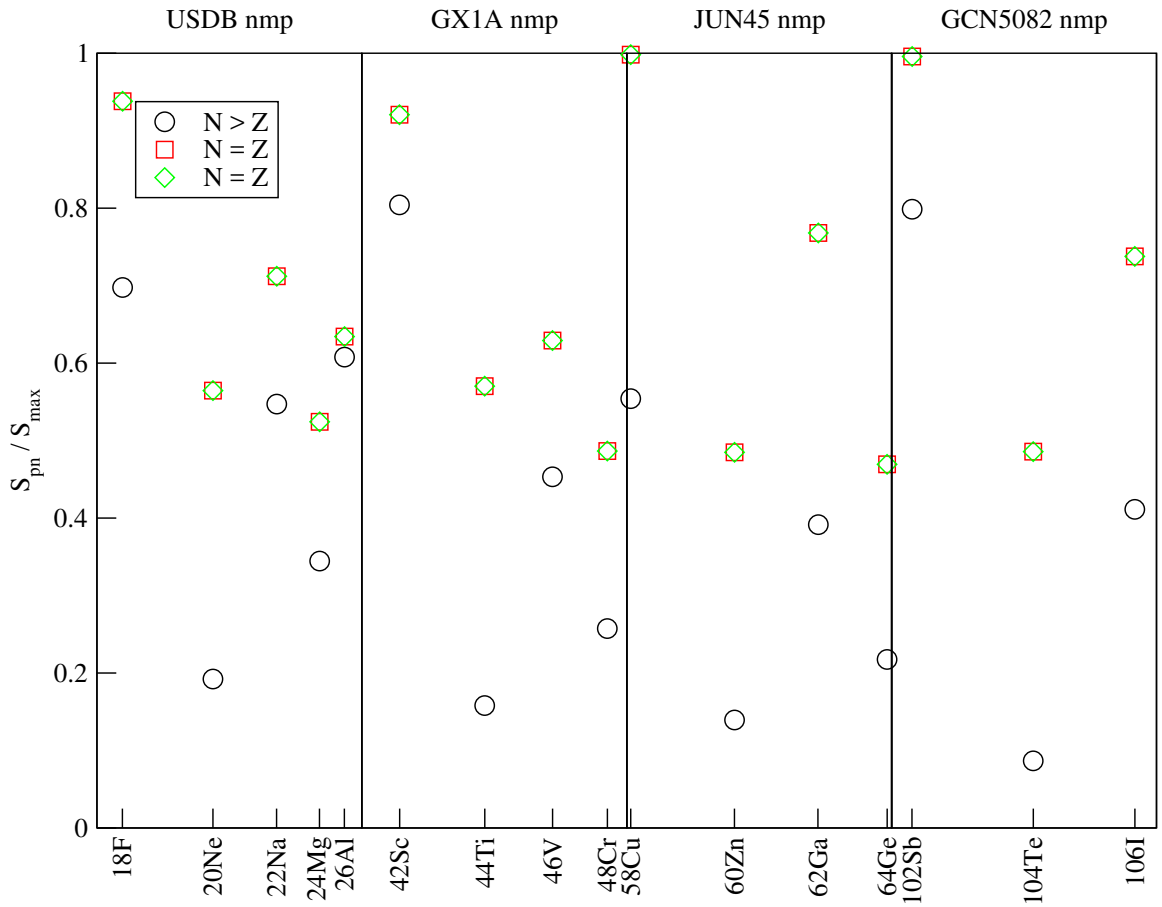

Figure 2. PN Entanglement Entropy in Particle Hole Conjugate Nuclei (Traceless)

In BIGSTICK, this means scaling the two-body interaction matrix elements by λ:

$$\lambda \langle ab|V^{(pn)}|cd\rangle \tag{41}$$

The scaling factor λ will be varied from zero, i.e. no proton-neutron interaction at all, to unity, i.e. a fully realistic calculation, and higher. We examined the relationship between the strength of the proton-neutron interaction and the relative proton-neutron entanglement entropy for the ground state of a number of nuclei. The entanglement entropy will be zero when λ is zero because in this case there is no interaction between the two nucleons. Essentially we have two separate and non-interacting model spaces. The entanglement entropy will increase as the strength of the interaction increases.

Again, Lanczos methods were used to compute only the low-lying states.

If our hypothesis that $N > Z$ nuclei converge faster in the proton-neutron formalism than $N = Z$ nuclei then we might expect certain behaviour in the S vs λ curves for $N > Z$ and $N = Z$ nuclei. In fact what we find is that the S vs λ curve for $N > Z$ nuclei falls below

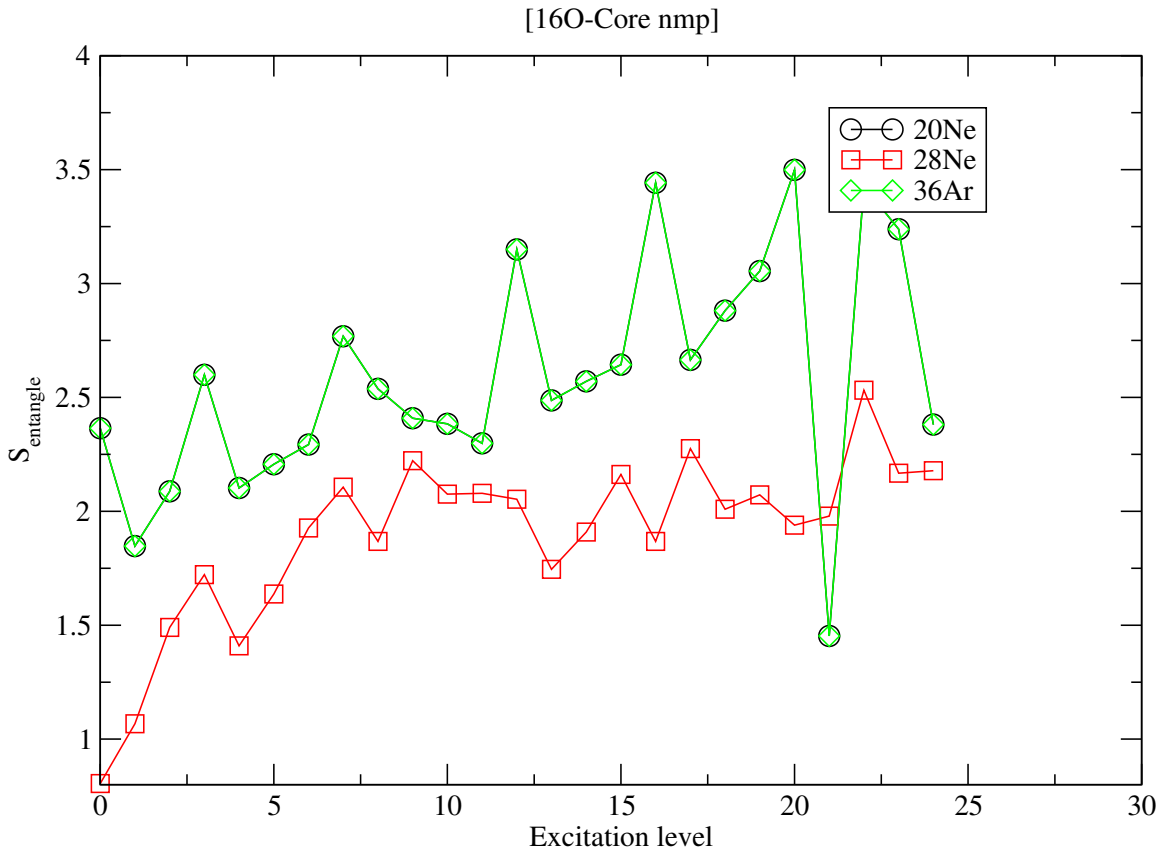

Figure 3. S vs Excitation Level: Ne

the one for $N = Z$ nuclei for nuclei of the same model space dimension. (Having the same model space dimension means that the two nuclei will also have the same maximum proton-neutron entanglement entropy.) This is accomplished by comparing nuclei which are particle-hole conjugates of each other.

Figure 6 shows the dramatic difference between the S versus λ curves of nuclei with $N = Z$ versus $N > Z$. $N > Z$ have significantly lower proton-neutron entanglement entropy for values of λ greater than zero up to about five to seven times the realistic scaling of the proton-neutron interaction.

PROTON-NEUTRON DECOMPOSITION

In the previous sections, we focused on the SVD eigenvalues, which allow us to predict whether or not it will be possible to find a more efficient representation of our nuclear wavefunctions. Now, we will examine a particular decomposition of wavefunctions. We will

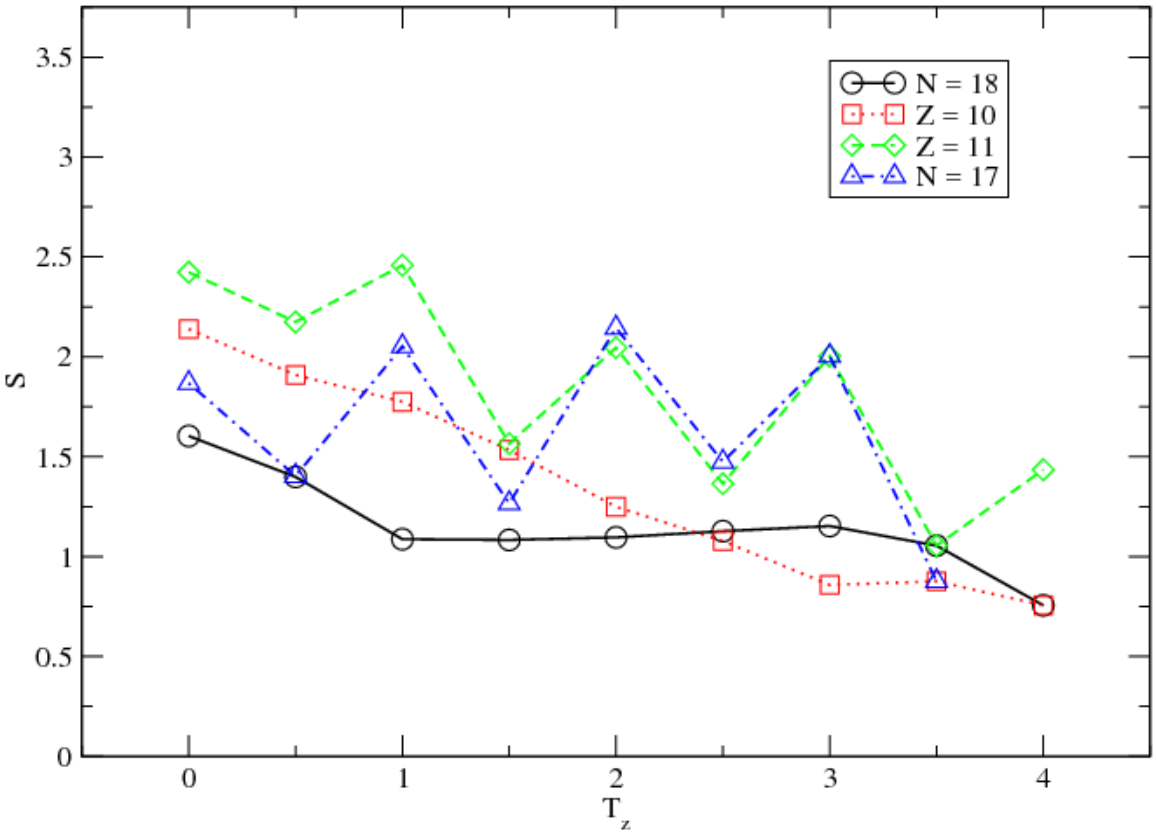

Figure 4. S vs Tz: SD Shell

be assuming that our Hamiltonian can be decomposed as

$$H = H_{p,pp} + H_{n,nn} + H_{pn} \tag{42}$$

where $H_{p,pp}$ contains all interactions between one or two protons, and similarly for $H_{n,nn}$ with neutrons, and that H_{pn} contains all interactions between a proton and a neutron. Then we call the eigenstates of the pure-proton Hamiltonian $|\pi\rangle$, as in

$$H_{p,pp}|\pi\rangle = E_p|\pi\rangle, \tag{43}$$

and the eigenstates of the pure-neutron Hamiltonian are equivalently define for $H_{n,nn}$ and $|\nu\rangle$.

Roughly speaking, our proposed truncation scheme is to compute the full Hamiltonian (42) in a basis build up from the coupled eigenstates of $H_{p,pp}$ and $H_{n,nn}$. It was therefore worth decomposing existing wavefunctions $|\Psi\rangle$ into the eigenstates of both pure-proton interaction operators and pure-neutron interaction operators. This will tell us how whether or not truncating a basis of coupled pure-proton and pure-neutron wavefunctions will be viable.

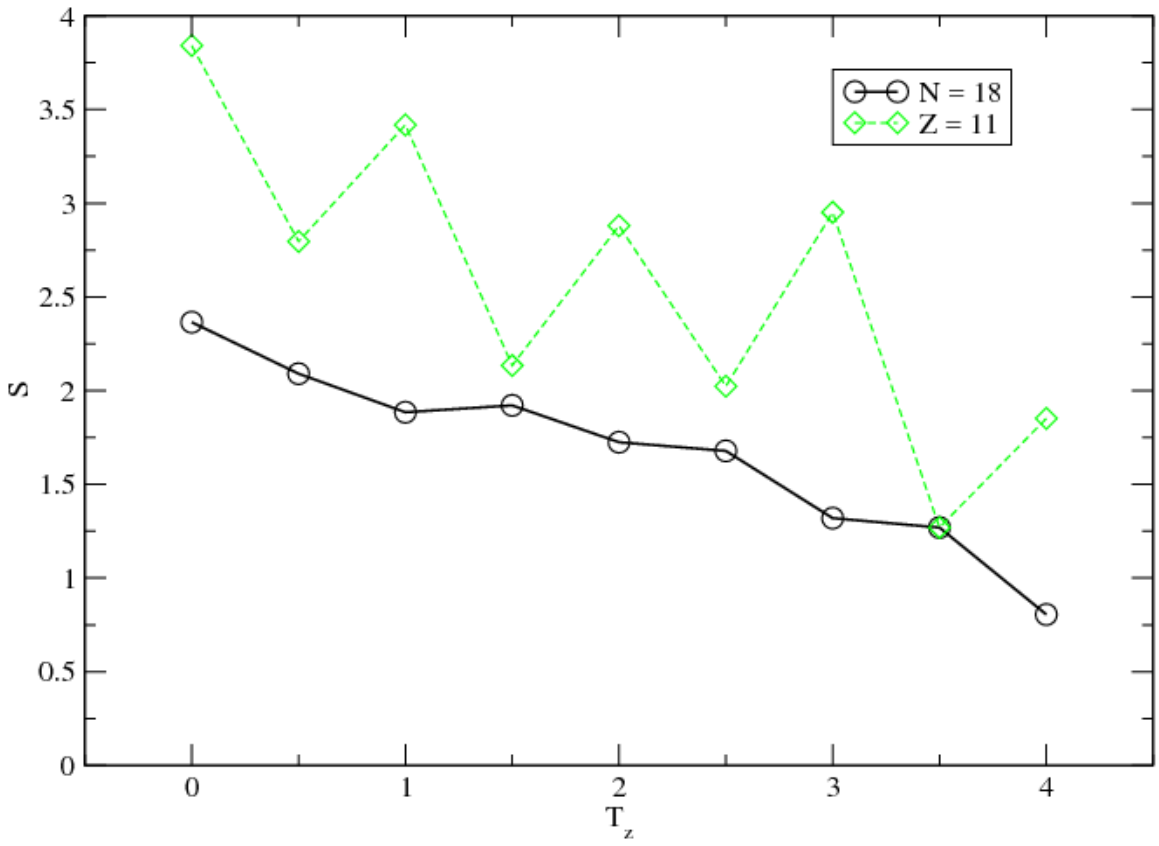

Figure 5. S vs Tz: SD Shell, Traceless

We project the expansion (23) onto the proton and neutron interaction eigenstates and extract the coefficients Ψ_{ab}. This was done using existing capabilities in BIGSTICK to compute transition strength functions. In particular I used the option to decompose wavefunctions onto scalar operators.[6] To do this, we first solve for the wavefunction $|\Psi\rangle$ for some nucleus. Then, BIGSTICK reads in the matrix elements for a proton-proton interaction,

$$V_{pp}|\pi_a\rangle = \epsilon^a_{pp}|\pi_a\rangle, \tag{44}$$

(or a neutron-neutron interaction) and uses its Lanczos capabilities to find low-lieing eigenstates $|\pi_a\rangle$ (or $|\nu_a\rangle$). Then, the nuclear wavefunction is projected onto these eigenstates in the following manner:

$$\begin{aligned} \langle\pi_a||\Psi\rangle &= \langle\pi_a| \sum_{a,b} \tilde{\Psi}_{ab}|\pi_a\rangle|\nu_b\rangle \\ &= \sum_b \tilde{\Psi}_{ab}|\nu_b\rangle. \end{aligned} \tag{45}$$

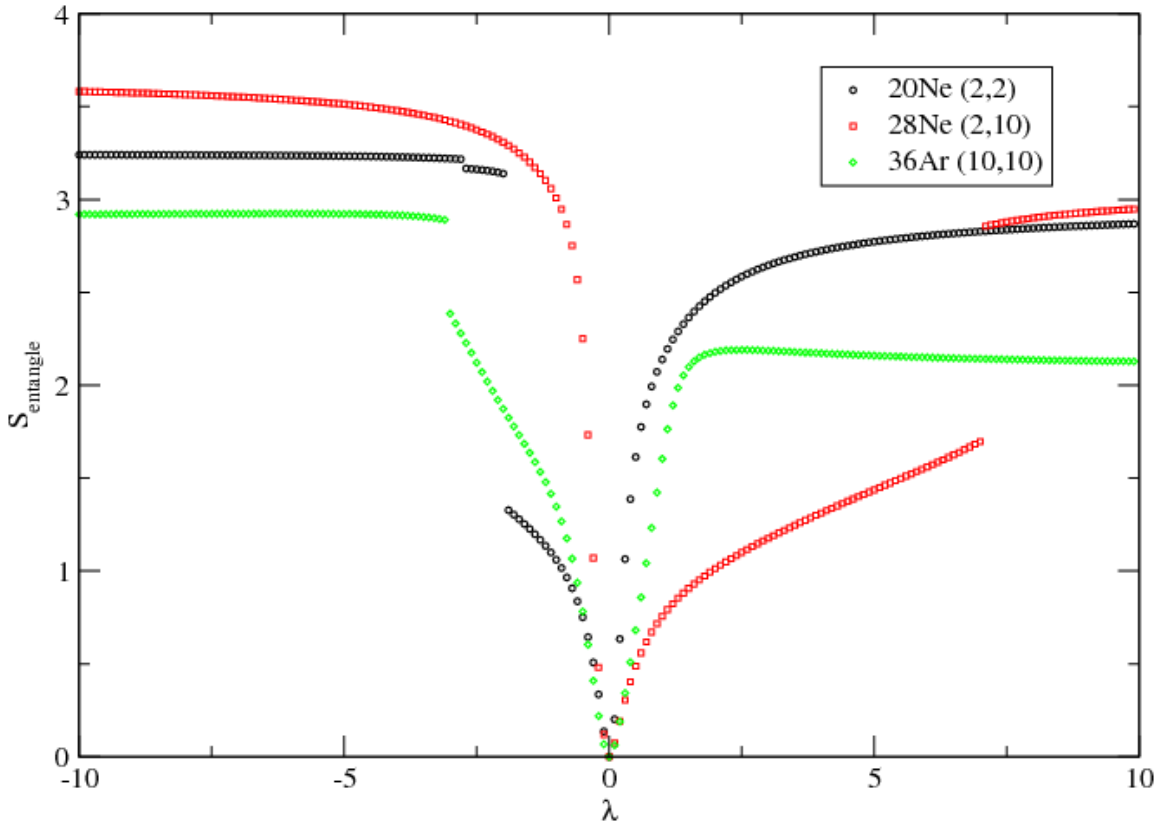

Figure 6. Entanglement Entropy: Ne

The strengths of these projections is then computed as

$$\begin{aligned}\langle\Psi||\pi'_a\rangle\langle\pi_a||\Psi\rangle &= \sum_b \tilde{\Psi}^*_{a'b}\tilde{\Psi}_{ab} \\ &= \sum_b^{N_{keep}} |\Psi_{ab}|^2 \\ &\equiv c_a^2.\end{aligned} \tag{46}$$

The quantities c_a^2 are the strengths of the projection of a wavefunction $|\Psi\rangle$ onto the proton-proton interaction eigenstate $|\pi_a\rangle$. Since we are assuming a set of normalized wavefunctions in our basis,

$$1 = \sum_a \langle\pi_a||\pi_a\rangle, \tag{47}$$

and thus the strengths c_a^2 are the fractions of the total wavefuntion $|\Psi\rangle$ contained in the state $|\pi_a\rangle$.

I decomposed nuclear wavefunctions in the sd-shell into their pure-proton and pure-neutron interaction strengths for the first few low-lieing eigenstates of the pure proton

and pure neutron two-body operators. An example is given in figure 37 and more are examples are provided in appendix C. These Proton-Neutron Decomposition plots were computed using the strength function options in BIGSTICK. The vertical axis is the strength of the decomposition onto the jth lowest eigenstate of either the proton-proton interaction of the neutron-neutron interaction. Each plots has four curves: two curves for each of the two particle-hole conjugate nuclei shown, one being the proton-proton (PP) decomposition and the other being the neutron-neutron (NN) interaction.

There are two important conclusions to be drawn from these plots. The first is that the strengths fall off rapidly in the first handful of states. This suggests than an expansion into pure-proton and pure-neutron eigenstates could a viable method for obtaining approximate wavefunctions. However it is already known that this is the case.[10–12] The second important feature is apparent when plotting the strength function decompositions for particle-hole conjugate nuclei on the same plot. We find that even though these pairs of nuclei have the same dimensions in their shell model spaces, nuclei for which $N > Z$ have strengths which are significantly lower than their $N = Z$ conjugates. This is further evidence that the same proposed truncation scheme may be even more effective in larger nuclei where $N > Z$.

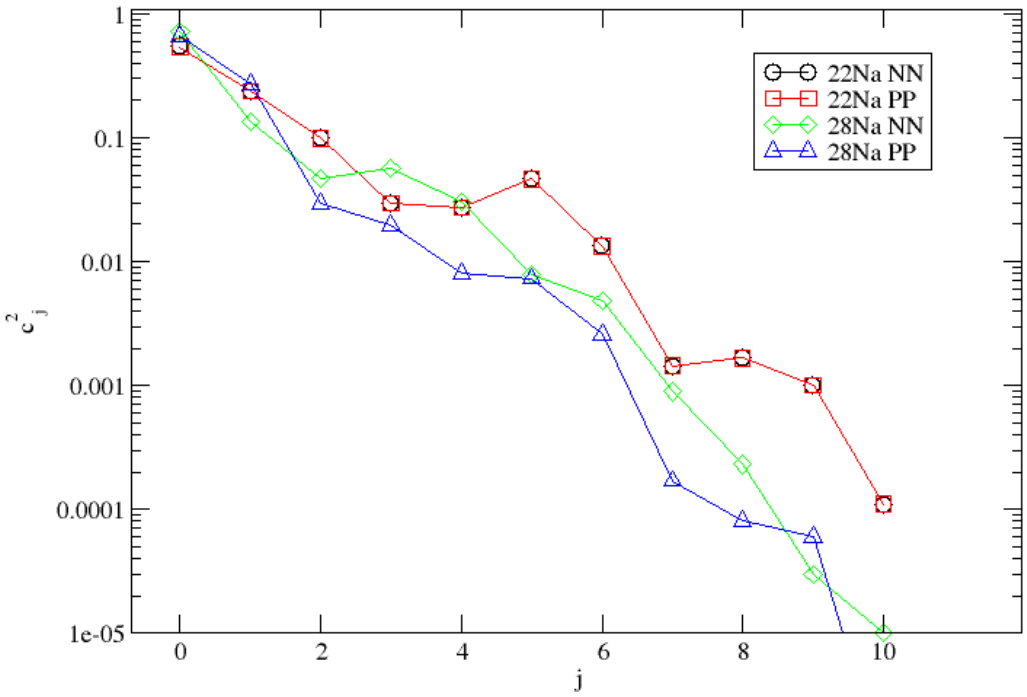

Figure 7. Proton-Neutron Decomposition: Na and PH-Conjugates

CHAPTER 3

PROTON NEUTRON COUPLING

We have shown that proton-neutron entanglement entropy is loosely correlated with the inverse of isospin, however it is not obvious why this is the case. In this chapter I summarize some of the attempts made to isolate the physics responsible for behaviour demonstrated in the previous chapter. In each of the first few sections, the Hamiltonian is modified to remove or isolate some aspect of the nuclear interaction.

In the last section of this chapter, a toy model is used in an attempt to reproduce the S vs λ curves from the previous chapter in a simple bipartide system with random guassian Hamiltonians.

MODIFIED NUCLEAR INTERACTIONS

(Zero Single Particle Energies) In this interaction we start with the fully realistic nuclear interaciton and then set the single particle energies equal to zero. In the many-body Hamiltonian,

$$H = \sum_{ij} \epsilon_{ij} a_i^\dagger a_i + \sum_{ijkl} a_i^\dagger a_j^\dagger V_{ijkl} a_k a_l \tag{48}$$

the single particle energies are ϵ_{ij}.

(Traceless Interaction) In this interaction we again start with the fully realistic nuclear interaction and then remove the monopole terms in the two-body interaction. These are terms of the form

$$P = \sum \tag{49}$$

And

(Attractive Quadrapole-Quadrapole) Instead of removing terms from the fully realistic nuclear interaction, the attractive quadrapole-quadrapole interaction was used.

(Pairing Interaction) However, a problem arose when computing entropies with lambda close to zero for certain large nuclei. In cases where the eigenstates are nearly degenerate, the Lanczos method performs poorly. This is because the Lanczos method is

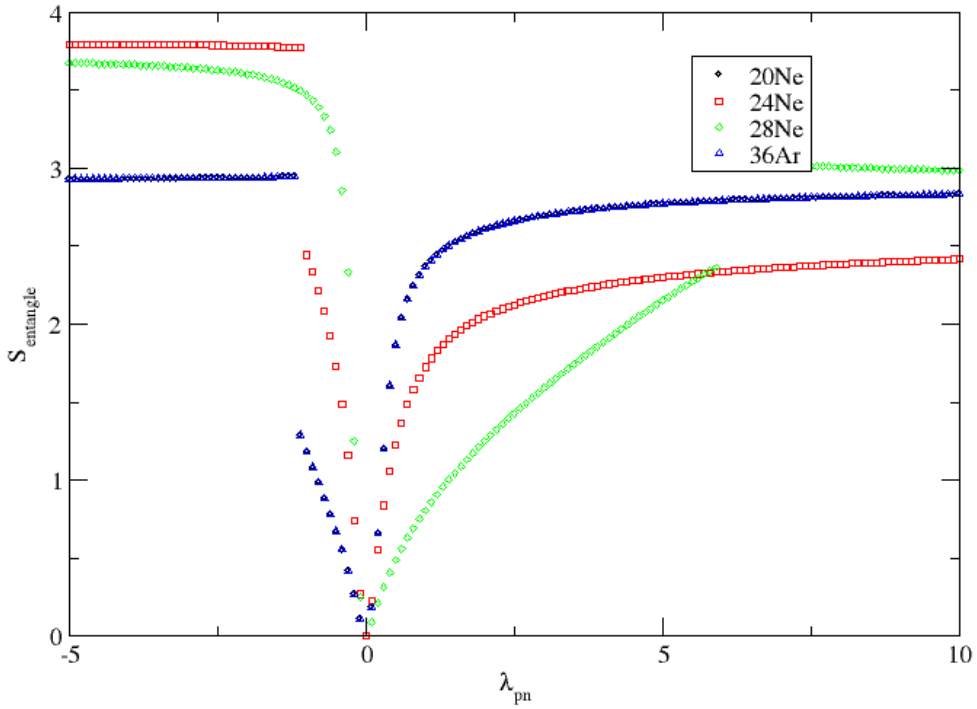

Figure 8. Traceless interaction: Ne

susceptable to loss of orthogonality of eigenstates due to numerical noise. In order to counteract this, the two-body interaction matrix elements were slightly modified. A very small random interaction was added to the matrix elements in order to desensitize the Lanczos algorithm to the degeneracies.

(Random interactions) We also ran several trials with particle-hole conjugate nuclei with random two-body interactions. This means that all of the physics is removed and all that remains are properties of the model space.

(Conclusion on the Source of the Weak Coupling) In each of the above trial interactions,

Toy Model

I constructed a toy model to investigate the behavior of entanglement entropy of coupled systems in an attempt to bettwe understand the behavior seen in real nuclei. The real space that we are dealing with in the case of nuclei is in a basis of slater determinants of

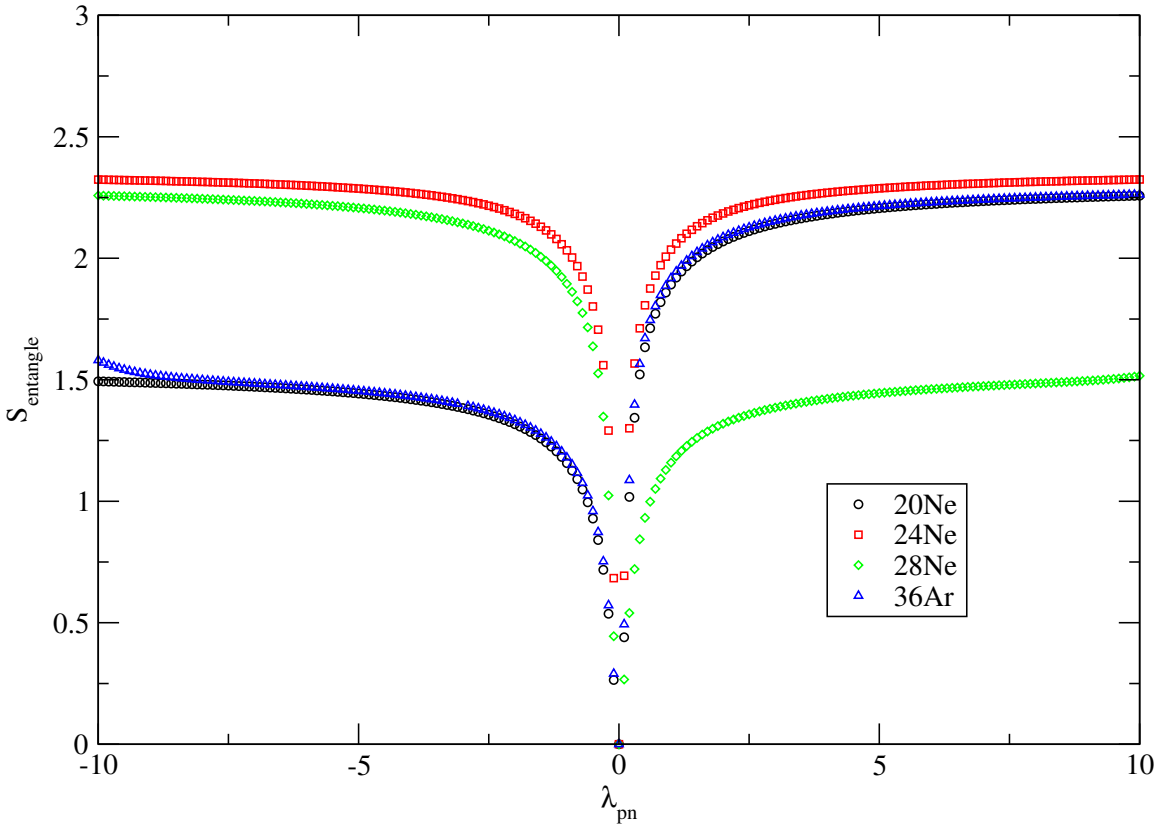

Figure 9. Attractive Quadrapole-Quadrapole Interaction: Ne and Conjugates

single particle states. This basis is made up of proton basis states and neutron basis states and it is possible to write operators which act exclusively on one or the other. In the toy model, I consider a single particle space A and a single particle space B, which together form a total mixed-particle space. Then we might choose a basis which is a product of basis states from the A space and the B space. i.e.

$$|i\rangle = |a\rangle|b\rangle = |a\rangle \otimes |b\rangle. \tag{50}$$

Thus a Hamiltonian operator in this combined, bipartide space could be written as

$$\hat{H} = \hat{H}_A + \hat{H}_B + \hat{H}_{AB} \tag{51}$$

where $\hat{H}_A = \hat{h}_a \otimes \hat{1}$ is an operator which acts purely in the A space, $\hat{H}_B = \hat{1} \otimes \hat{h}_b$ is an operator which acts purely in the B space and $\hat{H}_{AB} = \hat{V} \otimes \hat{W}$ is an operator which acts on both spaces.

Because what we are interested in is the behaviour of the system as a function of the coupling term $\hat{H}_{AB}$, I assume for convenience that we have already diagonalized $\hat{H}_A$ and $\hat{H}_B$.

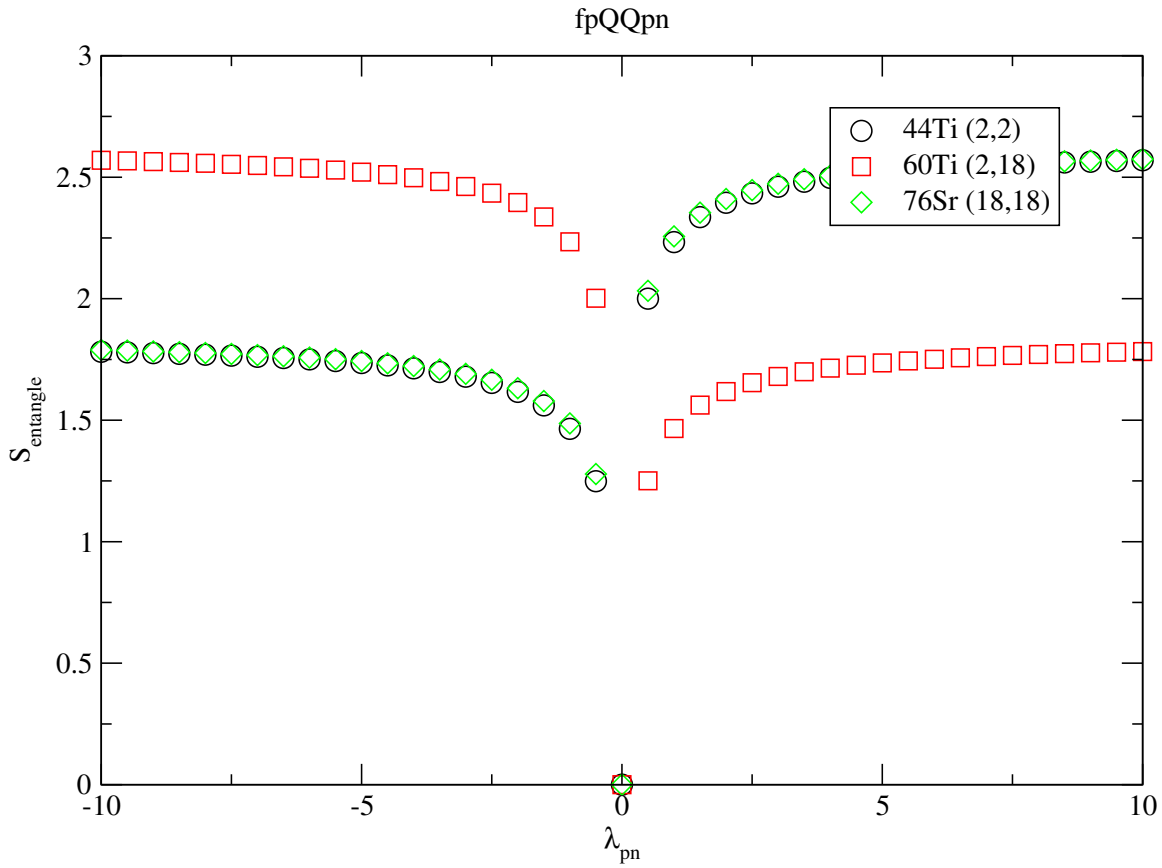

Figure 10. Attractive Quadrapole-Quadrapole Interaction: Ti and Conjugates

I choose to have identical single particle spaces with constant energy spacing. And so for this model I set

$$E_a \equiv \hat{h}_A|a\rangle = a\epsilon \tag{52}$$

for $a = 1, .., N$ and $\epsilon = const.$, and similarly for $\hat{H}_B$.

For $\hat{H}_{AB}$ I choose an operator which is the tensor product of an A-space operator $\hat{V}$ and a B-space operator $\hat{W}$. I am only interested in the behaviour of the system as a function of the strength of the interaction between the subsystems, so the exact structure of each subsystem is not important. Therefore, I simply choose to fill these two matrices with a random Guassian number generator. I symmetrically fill an $N \times N$ matrix with random numbers centered at zero with a standard deviation of 2σ for the diagonal matrix elements, and σ for the off-diagonal matrix, a standard practice for generating real, symmetric random matrices. Finally, I include a scaling factor λ which I can use to vary the relative size of the coupling term $\hat{H}_{AB}$.

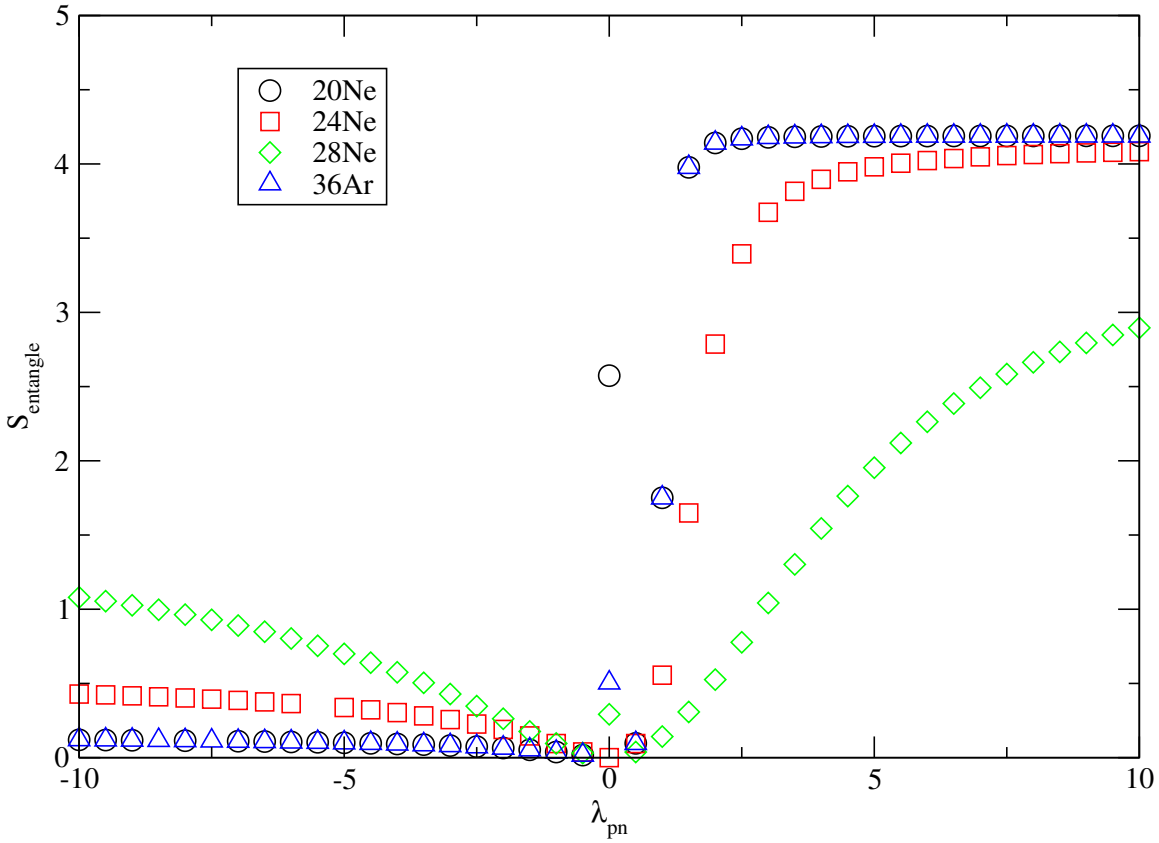

Figure 11. Attractive pairing interaction: Ne and PH-Conjugates

$$\hat{H}_{AB} = \lambda \hat{V} \otimes \hat{W} \tag{53}$$

It is now straightforward to calculate the matrix elements of the Hamiltonian. As above, let a, a' label the proton states and b, b' label the neutron states. These run from 1 to N. Now let $i = a + N(b-1)$ label the many-body state, which runs from 1 to N^2. Then

$$\langle i'|\hat{H}|i\rangle = H_{i',i} = \delta_{a'a}\delta_{b'b}(E_a + E_b) + \lambda V_{a'a} W_{b'b}. \tag{54}$$

$\mathbf{V}^p$ and $\mathbf{W}^n$ are real, symmetric, $N \times N$ random matrices with Gaussian distributions:

$$P(V_{aa'}) \sim exp\Big(- \frac{V_{aa'}^2}{2\sigma^2(1+\delta_{a'a})}\Big) \tag{55}$$

This says that our matrices are filled with random numbers with a Guassian distribution of σ for the off-diagonals and 2σ for the diagonals.

Once we diagonalize the model Hamiltonian, we want to quantify how the entanglement entropy is affected by the coupling- term scaling factor λ and by whether or not

we have identical or unique subspaces. Suppose that we diagonalize the Hamiltonian and that

$$\hat{H}|\psi\rangle_i = E_i|\psi\rangle_i \tag{56}$$

defines our N^2 eigenstates. Any given state can be written as

$$|\psi\rangle = \sum_i c_i|i\rangle = \sum_{a,b} c_{ab}|a\rangle|b\rangle. \tag{57}$$

The reduced density matrix ρ_A of the A-subsystem is the partial trace,

$$\rho_A = tr_a\ \rho \tag{58}$$

Or, in terms of our choice of indexing,

$$\rho_p(a, a') = \sum_{b=1}^{N} |a'b\rangle\langle ab| \tag{59}$$

We can now define the proton-neutron entanglement entropy of the state described by ρ to be the *von Neumann* entropy of the reduced density matrix ρ_p,

$$S_{pn} = -tr\rho_p\ log\rho_p. \tag{60}$$

If we first diagonalize ρ_p to find its N eigenvalues γ_i^2 then the entanglement entropy becomes

$$S_{pn} = -\sum_{i=1}^{N} \gamma_i^2\ ln\gamma_i^2. \tag{61}$$

This quantity measures the entanglement entropy, or the mixing of quantum bits, of the two subspaces in a given state of the Hamiltonian.

Here, $\epsilon = 1$, $\sigma = 1$, and two curves are plotted: one in which the random matrices V and W are the same and one in which they are different. We see that when the two subspaces are the same, the entanglement entropy tends towards some finite non-zero value. Whereas when the two subspaces are different, the entanglement entropy falls off to zero.

In this adaption of the model we start with two identical subspaces and then slowly change one of the subspaces to be different from the original. In doing so we can see that as the two subspaces diverge, the entanglement entropy of the system falls off from its maximum convergent value.

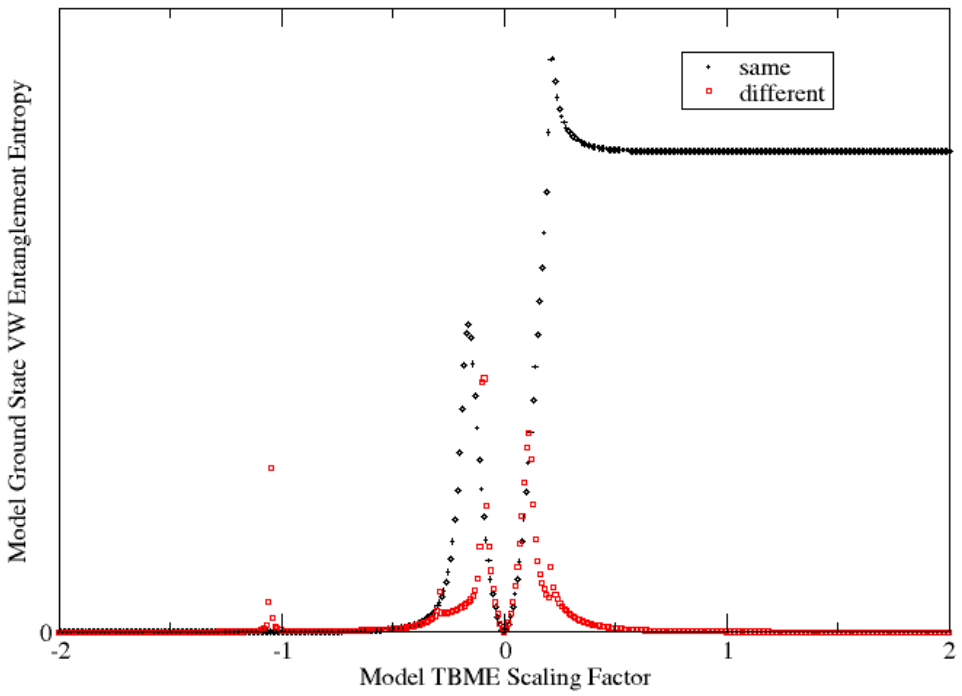

Figure 12. Toy Model: Ground State Proton-Neutron Entanglement Entropy as a function of the TBME Scaling Factor ($lambda$).

In an attempt to get convergence to non-zero entanglement entropies I suggested the following hamiltonian on the grounds that a constant term may prevent the entanglement entropy from falling off:

$$H_{i',i} = \delta_{a'a}\delta_{b'b}(E_a + E_b) + \lambda\big(V_{a'a}W_{b'b} + V_{a'a} + W_{b'b}\big) \tag{62}$$

Which implicitly is a hamiltonian of the form

$$H = E^V + E^W + \lambda(V \otimes W + V \otimes I + I \otimes W), \tag{63}$$

where E is diagonal. This produces the following results:

This version of the toymodel has the desired features of (1) going to zero at the origin and (2) converging to nonzero entanglement entropy. However the model lacks explicit physical interpretation.

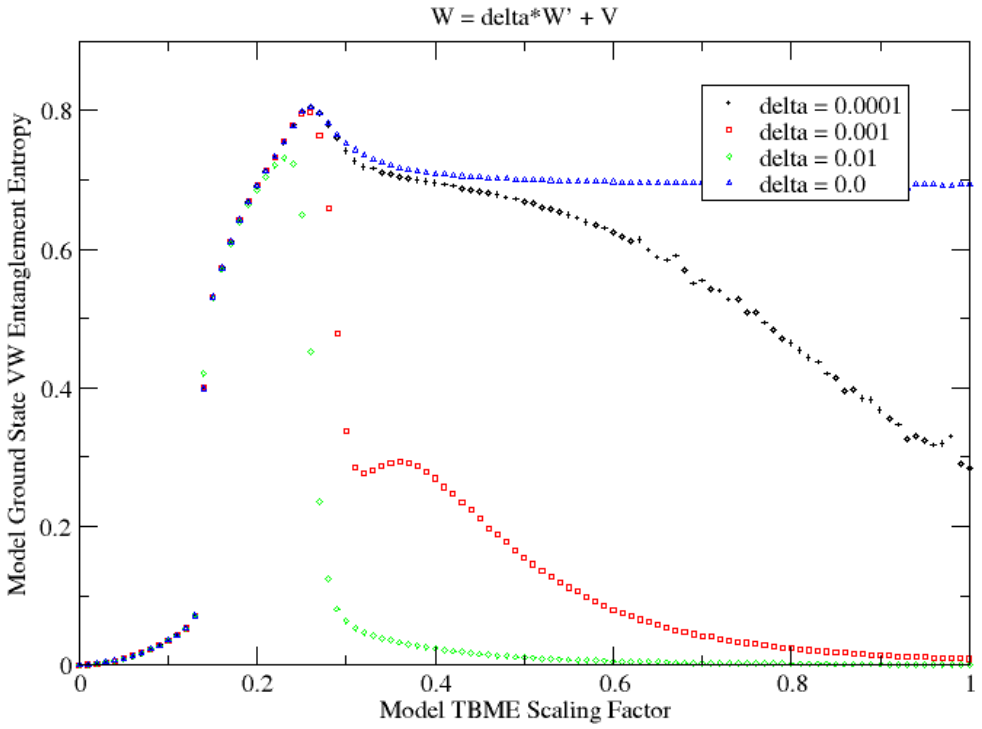

Figure 13. Toy Model: Perturbative variance of the subspaces.

$$H_{i',i} = \delta_{a'a}\delta_{b'b}(E_a + E_b) + \lambda\big(\sum_i V^i_{a'a} W^i_{b'b}\big) \tag{64}$$

Which is a hamiltonian of the form

$$H = E^{(V)} + E^{(W)} + \lambda(\sum_i V_i \otimes W_i) \tag{65}$$

This version of the toymodel has the following added features: (0) going to zero at the origin, (1) decreased dependence on the starting seed, (2) convergence to nozero entanglement entropies at large lambda for different subspaces and (3) fewer anomolous features (spikes in entanglement entropy). However the model still lackes discontinous jumps in entanglement entropy as seen in realistic calculations.

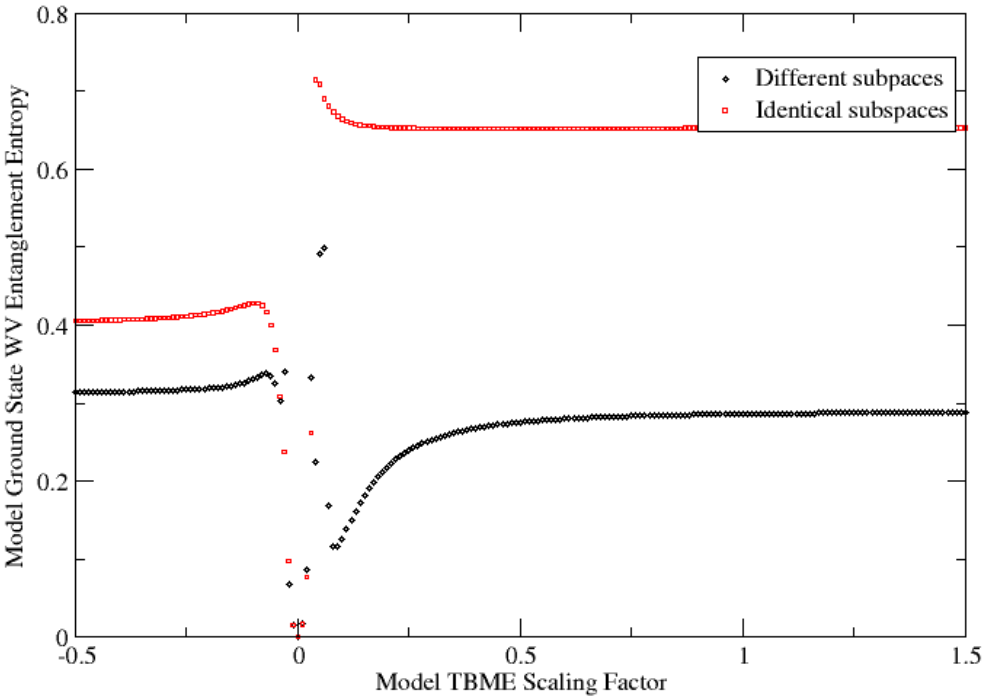

Figure 14. Toymodel: non-separable one-body terms.

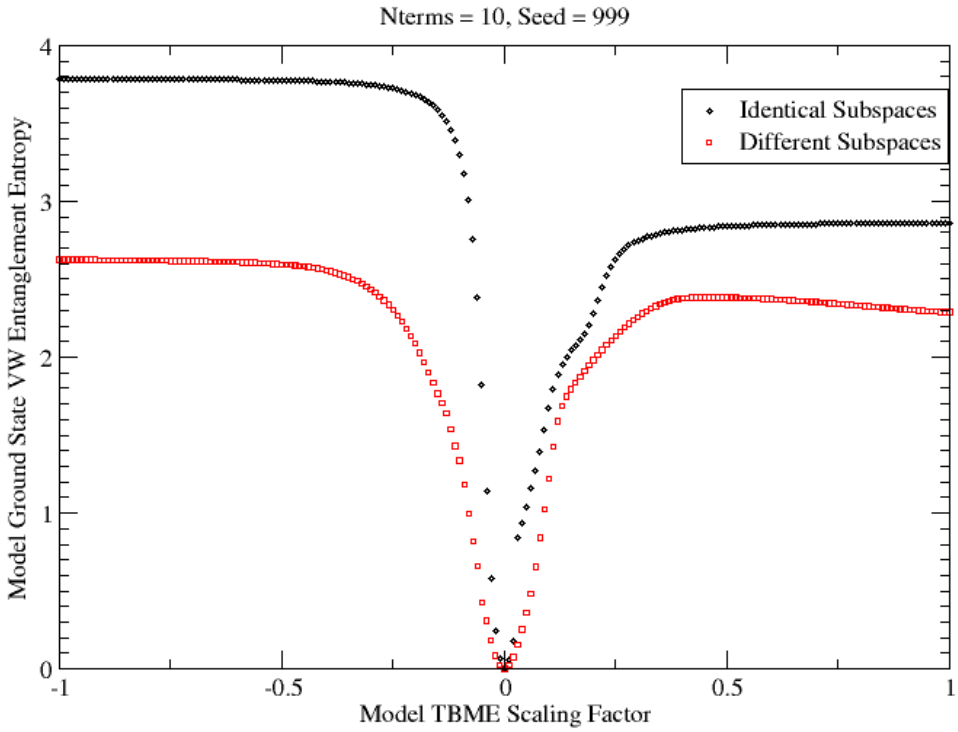

Figure 15. Toymodel: non-separable two-body terms.

CHAPTER 4

PNISM

Finally, we turn to the main subject of this thesis, our Proton-Neutron Interacting Shell Model (PNISM) code. We are motivated by the results of the previous chapters; we have seen that coupling between protons and neutrons is weaker in $N > Z$ nuclei. Since larger nuclei tend to be neutron rich, we have reason to believe that truncation of the model space in a weakly coupled proton-neutron basis might be an especially effective approximation. Our method will be to solve separately the neutron-neutron interaction and the proton-proton interaction, and to combine them with the coupled proton-neutron interaction in a truncated model space. We set out to write a code that takes eigenstates of the pure proton Hamiltonian and eigenstates of the pure neutron Hamiltonian, and creates a coupled proton-neutron basis from the results. The proton-neutron matrix elements are computed in this basis and added together with the pure-proton and pure-neutron matrix elements to recreate the full interaction.

This chapter will derive the equations used to cary out the calculation of the Hamiltonian and density matrices and the following chapter will discuss more of the details of the code itself.

THE HAMILTONIAN

We write the nuclear Hamiltonian in explicit proton-neutron formalism. That is to say, that the Hamiltonian is decomposited into a seperable sum of one-species two-body operators on the proton and neutron space, plus a two-body term that acts on both spaces.

To work in the second-quantization formalism we write the Hamiltonian as a sum of one body operators and two body operators in an expansion

$$\hat{H} = \hat{H}_{1b} + \hat{H}_{2b} + ... \tag{66}$$

as discussed in the introduction section on second quantization. Here we only deal with one and two body interactions.

It is usefule to define the two body creation operator as the following:[?]

$$\hat{A}^{\dagger}_{JM}(ab) \equiv [c^{\dagger}_{a} \otimes c^{\dagger}_{b}]_{JM} \tag{67}$$

Here the total angualr momentum J and the azimuthal or magnetic quantum number $M = J_z$ are set by the coupling of the two one-body creation operators. This done by Clebsch-Gordon coefficients:

$$[c^{\dagger}_{a} \otimes c^{\dagger}_{b}]_{JM} = \sum_{m_a m_b} (j_a m_a, j_b m_b | JM) \hat{c}^{\dagger}_{j_a m_a} \hat{c}^{\dagger}_{j_b m_b}. \tag{68}$$

With this definition of the two body creation operator, two-body states with proper normalization are[7]

$$|ab; JM\rangle \equiv \frac{1}{\sqrt{1+\delta_{ab}}} \hat{A}^{\dagger}_{JM}(ab)|0\rangle \tag{69}$$

The two-body part of the Hamiltonian is thus expressed

$$\begin{aligned} \hat{H_{2b}} &= \sum_{abcd} c^{\dagger}_{a} c^{\dagger}_{b} \langle ab|V|cd\rangle \hat{c}_c \hat{c}_d \\ &= \frac{1}{4} \sum_{abcd} \zeta_{ab}\zeta_{cd} \sum_{J} \langle ac; JM|V|cd; JM\rangle \sum_{M} A^{\dagger}_{JM}(ab) A_{JM}(cd) \end{aligned} \tag{70}$$

where $\zeta_{ab} \equiv \sqrt{(1+\delta_{ab})}$. This factorized form of the Hamiltonian is used by isospin conserving formalisms, e.g. BIGSTICK. Our next move is to change to an explicit proton-neutron decomposition. This means that the two-body interaction is separated into a triad containing a pure proton-proton interaction, a pure neutron-neutron interaction, and a pure proton-neutron interaction. This can be done by using the states $\frac{1}{\sqrt{2}}(|\pi\nu\rangle - |\nu\pi\rangle)$, $\frac{1}{2}(|\pi\nu\rangle + |\nu\pi\rangle)$,$|\pi\pi\rangle$, and $|\nu\nu\rangle$.

$$\hat{H}_{pp} = \frac{1}{4} \sum_{abcd} \zeta_{ab}\zeta_{cd} \sum_{J} V^{pp}_{J}(ab, cd) \sum_{M} \hat{A}^{\dagger}_{JM}(a_\pi b_\pi) \hat{A}_{JM}(c_\pi d_\pi) \tag{71}$$

THE BASIS

Suppose we have a Hamiltonian of the form

$$H = H_{pp} + H_{nn} + H_{pn}, \tag{72}$$

and that our many-body basis states are composed of (presumably normalized) coupled tensor products of proton and neutron states:

$$|J^{\pi_p}_{p}, \alpha_p\rangle \otimes |J^{\pi_n}_{n}, \beta_n\rangle \equiv |J^{\pi_p}_{p}, \alpha_p, J^{\pi_n}_{n}, \beta_n; J^{\pi}\rangle. \tag{73}$$

The proton-proton and neutron-neutron terms have matrix elements defined as

$$\langle J_p, \pi_p, \alpha_p | H_{pp} | J_p, \pi_p, \alpha_p \rangle \equiv h^{J_p^{\pi_p}}(\alpha'_p, \alpha_p) \tag{74}$$

and

$$\langle J_n, \pi_n, \alpha_n | H_{nn} | J_n, \pi_n, \alpha_n \rangle \equiv h^{J_n^{\pi_n}}(\beta'_n, \beta_n) \tag{75}$$

These are the single particle operators which will be starting off as solutions for the proton and neutron donor nuclei from BIGSTICK.

$$\begin{aligned} H_{pp}|J_p, \pi_p, \alpha_p\rangle &= E(\alpha_p)|J_p, \pi_p, \alpha_p\rangle \text{ and,} \\ H_{nn}|J_n, \pi_n, \alpha_n\rangle &= E(\alpha_n)|J_n, \pi_n, \alpha_n\rangle. \end{aligned} \tag{76}$$

Thus we have that

$$\begin{aligned} h^{J_p^{\pi_p}} &= \delta_{a'_p a_p} E(\alpha_p) \text{ and,} \\ h^{J_n^{\pi_n}} &= \delta_{b'_n b_n} E(\alpha_n). \end{aligned} \tag{77}$$

COUPLING

The proton-neutron two body interaction is factorized into the product of a two-body creation operator and a two-body anhiliation operator.

$$H_{pn} = \sum_{abcd} \sum_{J} V_J^{(pn)}(ab, cd) \sum_{M} A^\dagger_{JM}(a_\pi b_\nu) A_{JM}(c_\pi d_\nu). \tag{78}$$

To be able to calculate the matrix elements of H_{pn} from the density matrices of pure proton and pure neutron wave-functions and the proton-neutron interaction operator, we have to write (78) in a different form. First, some definitions. The two-body creation and annihilation operators are,[13] respectively,

$$\begin{aligned} A^\dagger_{JM} &= \sum_{m_a m_b} (j_a m_a, j_b m_b | JM) c^\dagger_{j_a m_a} c^\dagger_{j_b m_b} \\ A_{JM} &= \sum_{m_c m_d} (j_c m_c, j_d m_d | JM) c_{j_c m_c} c_{j_d m_d} \end{aligned} \tag{79}$$

We will refactor the proton-neutron interaction into terms that look like density matrices with some sort of vector-coupling coefficients. The generalized density operator is[14]

$$\rho_{K\mu}(a\tilde{c}) \equiv \sum_{m_a m_c} (j_a m_a, j_c - m_c | K\mu) c^\dagger_{j_a m_a} \tilde{c}_{j_c - m_c}. \tag{80}$$

Which, given the definition of the time-reversed operator,[15]

$$\tilde{c}_{j_c - m_c} = (-1)^{j_c - m_c} c_{j_c m_c}, \tag{81}$$

yields the equality

$$\rho_{K\mu}(a\tilde{c}) = \sum_{m_a m_c} (j_a m_a, j_c - m_c | K\mu)(-1)^{j_c - m_c} c^\dagger_{j_a m_a} c_{j_c m_c}. \tag{82}$$

The tilde over the index c reminds us that the time reversal operator was used but has no mathematical consequences. We will also need the following relationship[15] between vector-coupling coefficients and the *six-J symbol*,

$$(j_a m_a, j_b m_b | JM)(j_c m_c, j_d m_d | JM) = \sum_{K\mu} (-1)^{J+M} (-1)^{j_b - j_d + \mu} (2J+1) \begin{Bmatrix} j_a & j_b & J \\ j_d & j_c & K \end{Bmatrix} (j_a m_a, j_c - m_c | K\mu)(j_b m_b, j_d - m_d | K - \mu). \tag{83}$$

The six-J symbol is an invariant generalization of vector coupling coefficients. A brief introduction to vector coupling coefficients and six-J symbols are given in appendix A. Now we have what we need. We start again with (78) and sequentially apply the previously stated definitions and identities.

$$\begin{aligned} &\sum_M A^\dagger_{JM}(ab)\ A_{JM}(cd) \\ &\quad = \sum_M \sum_{m_a m_b m_c m_d} (j_a m_a, j_b m_b | JM)(j_c m_c, j_d m_d | JM) c^\dagger_{j_a m_a} c^\dagger_{j_b m_b} c_{j_d m_d} c_{j_c m_c} \\ &\quad = \sum_M \sum_{K\mu} (-1)^{J+M+j_b - j_d + \mu} (2J+1) \begin{Bmatrix} j_a & j_b & J \\ j_d & j_c & K \end{Bmatrix} (-1)^{-j_c + m_c - j_d + m_d} \rho_{K\mu}(a\tilde{c}) \rho_{K-\mu}(b\tilde{d}) \\ &\quad = \sum_{K\mu} (-1)^{J + j_b + j_c} (2J+1) \begin{Bmatrix} j_a & j_b & J \\ j_d & j_c & K \end{Bmatrix} (-1)^{\mu} \rho_{K\mu}(a\tilde{c}) \rho_{K-\mu}(b\tilde{d}) \end{aligned} \tag{84}$$

Note the cancelation of phases in the final equality, including by the general property that $(-1)^j = (-1)^{j+2n}$ and the condition that $M = m_a + m_b = m_c + m_d$. We define the following

dot product to further simplify the representation:

$$\begin{aligned}\rho_K(a\tilde{c})\cdot\rho_K(b\tilde{d}) &= \sum_{\mu}(-1)^K(2K+1)^{-1/2}(K\mu,K-\mu|00)\rho_{K\mu}(a\tilde{c})\rho_{K-\mu}(b\tilde{d}) \\ &= \sum_{\mu}(-1)^{-\mu}\rho_{K\mu}(a\tilde{c})\rho_{K-\mu}(b\tilde{d}).\end{aligned} \tag{85}$$

Where, again from Edmonds,[15] we applied the following identity for the case where we are coupling up to zero total angular momentum.

$$(K\mu,K-\mu|00) = (-1)^{K-\mu}(2K+1)^{-1/2}. \tag{86}$$

Thus the proton-neutron Hamiltonian can be written as

$$H_{pn} = \sum_{abcd}\sum_{J}V_J^{(pn)}(ab,cd)\sum_{K}(-1)^{J+j_b+j_c}(2J+1)\begin{Bmatrix} j_a & j_b & J \\ j_d & j_c & K\end{Bmatrix}\rho_K(a\tilde{c})\cdot\rho_K(b\tilde{d}) \tag{87}$$

which is a coupling of the proton and neutron density matrices through a coupling factor we will choose to label $W_K(ac,bd)$:

$$W_K(ac,bd) \equiv \sum_{J}(-1)^{J+j_b+j_c}(2J+1)\begin{Bmatrix} j_a & j_b & J \\ j_d & j_c & K\end{Bmatrix}V_J^{(pn)}(ab,cd). \tag{88}$$

Which gives us a form of the Hamiltonian that can be recognized as some potential $W_K(ac,bd)$ (containing coupling constants) times some refactorization of the two-body creation/anhilation operators $\rho_K(a\tilde{c})\cdot\rho_K(b\tilde{d})$:

$$H_{pn} = \sum_{abcd}\sum_{K}W_K(ac,bd)\rho_K(a\tilde{c})\cdot\rho_K(b\tilde{d}) \tag{89}$$

MATRIX ELEMENTS

Matrix elements can now be computed in our basis of coupled proton-neutron states using the above form of the Hamiltonian expressed in terms of density operators. Our full Hamiltonian is

$$H = H_p + H_{pp} + H_n + H_{nn} + H_{pn} \tag{90}$$

and the basis states are $|J_p^{\pi_p},\alpha_p,J_n^{\pi_n},\beta_n|J^\pi\rangle$. The first four terms are computed in BIGSTICK, which contribute the following matrix elements:

$$\delta_{J_n'J_n}\delta_{J_p'J_p}\Big(\delta_{\beta_n'\beta_n}h^{J_p}(\alpha_p',\alpha_p) + \delta_{\alpha_p'\alpha_p}h^{J_n}(\beta_n'\beta_n)\Big) \tag{91}$$

The final term H_{pn} is a sum of scalar product operators of two commuting tensor operators of the form

$$T(k) \cdot U(k) = \rho_K(a\tilde{c}) \cdot \rho_K(b\tilde{d}) \tag{92}$$

and can be computed in a coupled basis using a reduction to a product of operators in the uncoupled basis[15]

$$\begin{aligned}\langle j_1' j_2'; J'M'|T(k) \cdot U(k)|j_1 j_2; JM\rangle = \\ (-1)^{j_1+j_2'+J}\delta_{J'J}\delta_{M'M} \begin{Bmatrix} J & j_2' & j_1' \\ k & j_1 & j_2 \end{Bmatrix} \langle j_1'|T(k)|j_1\rangle\langle j_2'|U(k)|j_2\rangle\end{aligned} \tag{93}$$

In the case of (92), we will have our dependance on $\langle J_p^{\prime\pi_p'}, \alpha_p'|\rho_k(a\tilde{c})|J_p^{\pi_p}, \alpha_p\rangle$ and $\langle J_n^{\prime\pi_n'}, \beta_n'|\rho_k(b\tilde{d})|J_n^{\pi_n}, \beta_n\rangle$. These are just the proton and neutron density matrices represented in the basis of uncoupled proton and neutron states, respectively. Recalling that these uncoupled states are just the eigenstates of the pure proton and pure neutron parts of the full Hamiltonian, we see that these density matrices are the density matrices that will be produced by BIGSTICK when computing $H_p + H_{pp}$ and $H_n + H_{nn}$.

Then the proton-neutron hamiltonian matrix elements are

$$\begin{aligned}\langle J_p^{\prime\pi_p'}, \alpha_p', J_n^{\prime\pi_n'}, \beta_n'; J^\pi|\hat{H}_{pn}|J_p^{\pi_p}, \alpha_p, J_n^{\pi_n}, \beta_n; J^\pi\rangle = \\ \sum_{ac,bd}\sum_K W_K(ac,bd)(-1)^{J_p+J_n'+J} \begin{Bmatrix} J & J_n' & J_p' \\ K & J_p & J_n \end{Bmatrix} \\ \langle J_p^{\prime\pi_p'}, \alpha_p'|\rho_K(a\tilde{c})|J_p^{\pi_p}, \alpha_p\rangle\langle J_n^{\prime\pi_n'}, \beta_n'|\rho_K(b\tilde{d})|J_n^{\pi_n}, \beta_n\rangle\end{aligned} \tag{94}$$

This matrix is then solved using techniques from linear algebra. In PNISM, the user can either select the included Lanczos algorithm to solve for low lying states or to use the full diagonalization option using a routine from the LAPACK library, at the cost of increased run time.

The next major step is to calculate the one-body density matrices, which are used to calculate transition strengths. This is addressed in the next section.

ONE-BODY DENSITY MATRICES

A basic functionality of any configuration interaction code is the ability to calculate density matrices. The most general definition of a density matrix is

$$\rho_k^{f,i}(ab) = \langle\Psi_f|[c_a^\dagger \otimes c_b]_k|\Psi_i\rangle, \tag{95}$$

which finds its use in the calculation of operator matrix elements

$$\langle \Psi_f | \hat{O} | \Psi_i \rangle = \sum_{ab} \rho_k^{f,i}(ab) \langle a | \hat{O} | b \rangle. \tag{96}$$

In order to calculate the density matrix elements between the eigenstates of the proton-neutron hamiltonian, which are output from PNISM in the basis of coupled proton and neutron wavefunctions, we need to be able to write (95) in terms of the density matrices provided by BIGSTICK. These, however, are computed in the basis of pure proton and pure neutron wavefunctions. This section walks through the derivation of the one-body density matrix elements for our eigenstates in terms of the one-body density matrices from the donor wavefunctions.

The matrix elements of a tensor product operator in a basis of coupled states are[15]

$$\begin{aligned} &\langle j_1' j_2'; J' | [\hat{T}_{k_1} \otimes \hat{U}_{k_2}]_K | j_1 j_2; J \rangle \\ &= [J'][K][J] \begin{Bmatrix} j_1' & j_1 & k_1 \\ j_2' & j_1 & k_2 \\ J' & J & K \end{Bmatrix} \langle j_1' | \hat{T}_{k_1} | j_1 \rangle \langle j_2' | \hat{U}_{k_2} | j_2 \rangle. \end{aligned} \tag{97}$$

If either $\hat{T}_{k_1}$ or $\hat{U}_{k_2}$ is the identity operator, as is the case for the one-body density matrices, then this expression further simplifies to

$$\begin{aligned} &\langle j_1' j_2'; J' | [\hat{T}_{k_1}] | j_1 j_2; J \rangle \\ &= \delta_{j_2' j_2} (-1)^{j_1' + j_2 + J + K} [J'][J] \begin{Bmatrix} j_1' & J' & j_2 \\ J & j_1 & k \end{Bmatrix} \langle j_1' | \hat{T}_k | j_1 \rangle \end{aligned} \tag{98}$$

and similarly for $\hat{U}_{k_2}$.

Thus we can find the proton density matrix elements in the coupled basis in terms of the density matrices in the uncoupled basis as

$$\begin{aligned} &\langle j_\pi' j_\nu'; J' | [\pi_a^\dagger \otimes \pi_c]_K | j_\pi j_\nu; J \rangle \\ &= \delta_{j_\nu' j_\nu} (-1)^{j_\pi' + j_\nu + J + K} [J'][J] \begin{Bmatrix} j_\pi' & J' & j_\nu \\ J & j_\pi & k \end{Bmatrix} \langle j_\pi' | [\pi_a^\dagger \otimes \pi_c]_K | j_\pi \rangle \end{aligned} \tag{99}$$

The delta functional comes from the identity operator on the neutron space, and the orthogonality of the basis states. If more quantum numbers were included, delta functionals would have to be added. Similarly, for the neutron density operator $[\nu_b^\dagger \otimes \nu_d]_K$ we have

$$\begin{aligned}
&\langle j'_\pi j'_\nu; J'|[\nu_b^\dagger \otimes \nu_d]_K|j_\pi j_\nu; J\rangle \\
&= \delta_{j'_\pi j_\pi}(-1)^{j_\pi+j_\nu+J'+K}[J'][J] \begin{Bmatrix} j'_\nu & J' & j_\pi \\ J & j_\nu & k \end{Bmatrix} \langle j'_\pi|[\pi_a^\dagger \otimes \pi_c]_K|j_\pi\rangle.
\end{aligned} \tag{100}$$

Note that this is not as simple as exchanging π and ν.

Finally, to get the expression for the density matrix for our coupled-state solutions, recall that our states Ψ_f and Ψ_i in (95) are solutions to

$$\hat{H}|\Psi\rangle = E|\Psi\rangle \tag{101}$$

and are given in the basis of coupled proton-neutron states. Each state can be written as

$$|\Psi\rangle = \sum_\alpha c_\alpha |j_\pi j_\nu; J\rangle_\alpha. \tag{102}$$

Combining this expression (102) and the relation (99) with our definition (95), we obtain the desired result

$$\begin{aligned}
\rho_k^{f,i}(\pi_a\pi_c) &= \langle \Psi_f|[\pi_a^\dagger \pi_c]_k|\Psi_i\rangle \\
&= \sum_{\alpha\beta} c_\alpha^f c_\beta^i \langle j_\pi^\alpha j_\nu^\alpha; J^f|[\pi_a^\dagger \pi_c]_k|j_\pi^\beta j_\nu^\beta; J^i\rangle \\
&= \sum_{\alpha\beta} c_\alpha^f c_\beta^i \delta_{j_\nu^\alpha j_\nu^\beta}(-1)^{j_\pi^\alpha + j_\nu^\beta + J^i + K}[J^f][J^i] \begin{Bmatrix} j_\pi^\alpha & J^f & j_\nu^\beta \\ J^i & j_\pi^\beta & k \end{Bmatrix} \langle j_\pi^\alpha|[\pi_a^\dagger \pi_c]_K|j_\pi^\beta\rangle.
\end{aligned} \tag{103}$$

The neutron one-body density matrix has identical structure.

This conludes the paper and pencil calculations necessary to write the proton neutron interacting shell model, PNISM. We have the expression for both the Hamiltonian matrix elements in terms of quantities which can be obtained from solutions from BIGSTICK (or any properly formatted results from an interacting shell model code), and the one-body density matrices which are used to compute transition rates. Equation (94) along with (88) and (103) are the actual equations coded up in PNISM.

CHAPTER 5

COMPUTATION

OVERVIEW OF PNISM

PNISM is a post processing code for BIGSTICK and relies on results from BIGSTICK in order to compute nuclear wavefunctions. Johnson wrote the majority of the code in subroutines responsible for reading in formatted results from BIGSTICK output files, as well as for constructing the basis. I aided in a few bugfixes in the modules responsible for reading in the density matrices (see "Challenges and Speedup"). I then wrote the majority of the code responsible for computing the proton-neutron-coupled-Hamiltonian H_{pn}, for solving the Hamiltonian, for computing the density matrices, and for writing the results to file. In this section I outline the flow of information and the algorithms and computations carried out. I leave out most of the theoretical details, as this is discussed in previous chapters, and focus on the computation.

The explicit proton-neutron formalism Hamiltonian is

$$H = H_p + H_{pp} + H_n + H_{nn} + H_{pn}. \tag{104}$$

BIGSTICK is used to solve $H_p + H_{pp}$ and $H_n + H_{nn}$ independently, before the PNISM runtime. Then PNISM reads in the following:

- The single particle orbit space (e.g. sd.spo)
- The two-body matrix elements $\langle ab, JT|V|cd, JT\rangle$
- The energy levels and quantum numbers from both $H_p + H_{pp}$ and $H_n + H_{nn}$
- The density matrices from both $H_p + H_{pp}$ and $H_n + H_{nn}$, from solutions of different $M \equiv J_z$ values

After reading the all of the necessary resources, PNISM creates the basis by coupling the eigenstates of $H_p + H_{pp}$ and $H_n + H_{nn}$ up to states with good total angular momentum. Then,

the array containing $W_K(ac, bd)$ is computed from the two-body matrix elements and with six-J symbols which are either computed on the fly or read in from a table stored on disk. Then, the largest portion of runtime takes place when the Hamiltonian matrix elements are computed using the diagonalized matrix elements of $H_p + H_{pp}$ and $H_n + H_{nn}$, the array containing $W_K(ac, bd)$, the density matrices of $H_p + H_{pp}$ and $H_n + H_{nn}$, and again the six-J symbols. PNISM then diagonalizes the Hamiltonian matrix, thus solving the many-body Schrodingder equation. The resulting quantum numbers and eigenvectors are used to calculate the one-body density matrices and the results are written to a file in the same format as would be produced by BIGSTICK.

READING IN DENSITY MATRICES

PNISM must read in multiple solutions from BIGSTICK for the same proton/neutron configuration because BIGSTICK is an M-scheme code. A solution for a given M value will have some number of zero density matrix elements due to symmetries in the Clebsch Gordan coefficients. Density matrices from BIGSTICK are actually reduced density matrices. A reduced matrix element of a tensor operator is a way to represent the matrix element of an operator without regard to the orientation in space. This is accomplished with the Wigner-Eckart theorem, which I will not explain here. The result is that for a tensor operator $\hat{O}_K M$,

$$\begin{aligned}\langle J_f M_f|\hat{O}_{KM}|J_i M_i\rangle &= [J_f]^{-1}(J_i M_i K M|J_f M_f)\langle J_f|\hat{O}_k|J_i\rangle \\ &= (-1)^{J_f - M_f}\begin{Bmatrix} J_f & K & J_i \\ -M_f & M_K & M_i \end{Bmatrix}\langle J_f|\hat{O}_k|J_i\rangle\end{aligned} \tag{105}$$

Where $[j] \equiv \sqrt{2j+1}$ and the six-argument array is the Six-J symbol. $\langle J_f|\hat{O}_k|J_i\rangle$ are the reduced density matrix elements of $\langle J_f M_f|\hat{O}_{KM}|J_i M_i\rangle$. A basic symmetry of vector coupling coefficients is[15]

$$(j_a m_a j_b m_b|JM) = (-1)^{j_a + j_b - J}(j_b m_b j_a m_a|JM) \tag{106}$$

It can be shown by applying time reversal symmetries to equation (106) that[15]

$$(j_a m_a j_b m_b|JM) = (-1)^{j_a + j_b - J}(j_a - m_a j_b - m_b|J - M). \tag{107}$$

Thus if $m_a = m_b = M = 0$, the coefficient must be zero. This creates a problem for our reduced density matrices since we divide by this quantity. To recover the missing density

matrix elements, we simply recompute $H_p + H_{pp}$ and $H_n + H_{nn}$ for another value of M. In practice, only $M = 0$ and $M = 1$ solutions are required to obtain nearly the entire solution. PNISM will only read in nonzero density matrix elements.

$M = 1$ basis states cannot have $J = 0$ total angular momentum (the total angular momentum can't be less than its z-component). Thus $M = 1$ solutions from BIGSTICK are missing all $J = 0$ solutions. It is therefore necessary to read in $M = 0$ solutions first when setting up the basis. The overall phase of the density matrix elements first read in are taken to be the convention. An important obstacle that had to be overcome resulted from a symmetry of quantum mechanics. When solving the Schrodinger equation, the overall sign of the wavefunction is not important, since it does not effect any observables. However, the relative phase between two wavefunctions is important, so care must be taken to establish self consitant phases. Because PNISM inputs solutions from BIGSTICK, the phase between two separate solutions, say, for two different $J_z \equiv M$ values (BIGSTICK is an M-scheme code) can differ. It is vital to check the relative phase between density matrices from different choices of M. Neglecting this will result in unforseen cancelations and a failure to recreate the Hamiltonian. After the initial density matrix that PNISM reads in, new density matrix elements for a given basis state combination are compared against density matrix elements that have already been read in. If an inconsitent phase is encountered, the read in is restarted for that basis state combination and the phase is adjusted accordingly.

COUPLED PROTON-NEUTRON BASIS

Once all of the resources are read in, PNISM computes the proton-neutron coupled Hamiltonian. The details of the computation are found in the previous chapter. A significant property of PNISM is that it works in a J-scheme basis as opposed to an M-scheme basis. The basis is composed of coupled proton-neutron states with good angular momentum quantum numbers J. This means that the Hamiltonian matrix elements can be divided up into groups of constant total angular momentum J. It is known that the M-scheme basis is more efficient than the J-scheme basis. So why work in the J-scheme?

So far all we have done is to solve the nuclear Hamiltonian in a basis of coupled proton and neutron states with good total J. The computational advantage to this procedure lies in the prospect of truncating the model space. This means that the eigenstates of the

Hamiltonian are taken to be

$$|\phi\rangle = \sum_{i_p}^{Q<<N^p} \sum_{i_n}^{Q<<N^n} c_{i_p i_n} |i_p\rangle \otimes |i_n\rangle. \tag{108}$$

$|i_p\rangle = |\pi\rangle$ and $|i_n\rangle = |\nu\rangle$ are proton and neutron wavefunctions which are eigenstates of the proton-proton and neutron-neutron Hamiltonians, respectively. If we were to truncate the basis in an M-Scheme procedure, then our solutions would not be guarenteed to have good total angular momentum. To see why, consider the following example for a two state system. Imagine a basis with two states $\frac{1}{\sqrt{2}}(|z;+\rangle + |z;-\rangle)$ and $\frac{1}{\sqrt{2}}(|z;+\rangle - |z;-\rangle)$. If we were truncate to just one of either of these states, then any solution in the truncated basis could not be an eigenstate of $\hat{S}_z$. Similarly, a truncated M-scheme basis is not guarenteed to have good total angular momentum. Therefore, we choose a basis with good total angular momentum so that even once we truncate the basis we are guarenteed to get solutions with good total angular momentum.

SYMMETRIES

A number of basic symmetry relations were used to speed up caclulations. The most obvious symmetry being the Hermiticity of the Hamiltonian matrix elements. After basic testing, only the diagonal and upper triangular portion of the Hamiltonian is computed independently. The remaining matrix elements are then copied over across the diagonal.

A similar but slightly less trivial method was used to compute the one-body density matrices. The one-body density matrices respect the so called time reversal symmetry:

$$\langle \Psi_f || [\hat{c}_a^\dagger \otimes \hat{c}_b]_k | \Psi_i \rangle = (-1)^{j_a - j_b + j_i - j_f} \langle \Psi_i || [\hat{c}_b^\dagger \otimes \hat{c}_a]_k | \Psi_f \rangle \tag{109}$$

This means that we only need to compute the upper triangular (in the a,b indices) elements of the one-body density matrices. The rest can be computed via the relation given in (109).

NUMERICAL METHODS

The primary eigensolver used in PNISM is SSYSEV from the LAPACK [ref] library. PNISM has the option to either use SSYEV directly, or to use a custom Lanczos solver. The Lanczos solver is useful when only extremal eigenstates are sought. The Lanczos solver uses a straightforward lanczos iteration subroutine written by another graduate student, Ryan [Lastname]. The Lanczos method is discussed in Appendix A. In my implementation, I use an

iterative process to incrementally increase the number of Lancozs iterations until some fixed number of eigenvalues converges. Convergence is measured by a somewhat crude criterion:

$$Crit = \frac{1}{N_{keep} - 1} \sum_{i=1}^{N_{keep}} |\lambda_i^{Current} - \lambda_i^{Previous}|. \tag{110}$$

Here, λ_i are the first N_{keep} eigenvalues produced by solving the Lanczos matrix. The process is said to have converged when the value of $Crit$ falls below some constant. In PNISM the value 0.001 is used. This is a similar convergence criterion used in BIGSTICK and tests show that it converges to the correct values.

In some cases where the total dimension of the matrix is small compared to the number N_{keep}, the $Crit$ value will fail to become small enough, even when the number of lanczos iterations is maximum (equal to the dimension of the matrix). When this happens an flag is thrown and the code runs LAPACK instead.

CHALLENGES AND SPEEDUPS

Computing the matrix elements of the Hamiltonian in PNISM takes most of the overall runtime. Several actions were take to help reduce this runtime. Using the Unix profiling tool GPROF, I found that a large percentage of compute time was used in calling the function used to compute Six-J symbols, a function with six arguments and calls to other subfunctions within an external library. In order to reduce the time used computing Six-J symbols, I wrote a small code to create a table of Six-J tables called sj2i.f90. The code asks the user for six inputs, the six maximum value of angular momentum, Jmax, to compute the Six-J symbol for. The Six-J symbols are then computed for all combinations of argument values from zero to Jmax and written to a file with the following format:

```
j1 j2 j3 j4 j5 j6 six-j(j1,j2,j3,j4,j5,j6)
```

In order to save disk space and I/O time, the file is written as an 'unformatted', non-ASCII file. Before any computation, PNISM reads the contents of the file into an array:

```
sj2i_table(j1+1,j2+1,j3+1,j4+1,j5+1,j6+1)
                        = six-j(j1,j2,j3,j4,j5,j6)
```

At the time when this document was written, the entire Hamiltonian for all total J values is computed sequentially, and then solved afterward. This is a waste of memory since

each total J Hamiltonian is independent and can be solved before the next is computed and committed to memory. A future project will be to solve each matrix as soon as it is computed. This should reduce the maximum memory requirements by approximately a factor equal to the total number of total-J values requested. I.E. if computing J-total from 0 to 10 then as much as one-tenth the total memory will be required with little cost to runtime.

CHAPTER 6

RESULTS

GROUND STATE CONVERGENCE

The following results demonstrate the exponential convergence of the ground state energy as a function of the number of states retained, for nuclei where a full diagonalization is possible even on a laptop. Results are given for sample nuclei in both the sd shell and the pf shell. When all of the states are retained, the results are exactly equal to those of BIGSTICK.

EXCITATION SPECTRA

The following results demonstrate the convergence of low-lying excitations in the sd and pf shells. When all of the states are retained, the results are exactly equal to those of BIGSTICK. Qualitatively one can observe that $N > Z$ nuclei tend to converge faster than $N = Z$ nuclei.

TRANSITION STRENGTHS

The previous sections dealt with the convergence of the eigenvalues, the excitation spectra. In order to examine the convergence of the wavefunctions, we calculate the transition strengths for $M1$ transistions. As expected, when all of the states are included, the results converge to those of BIGSTICK.

CAPSTONE CALCULATIONS

These calculations are meant to push PNISM to its limits to demonstrate its use. We study three nuclei, Ni56, Ni60 and Ge64 in the () model space, showing convergence plots of the ground state energy, and excitation plots for the first few low-lying excitation energies.

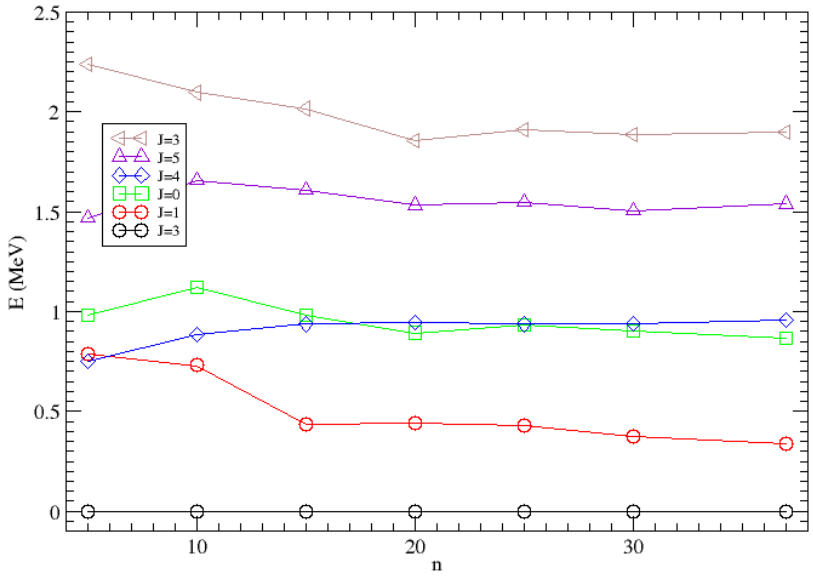

Figure 16. 22Na

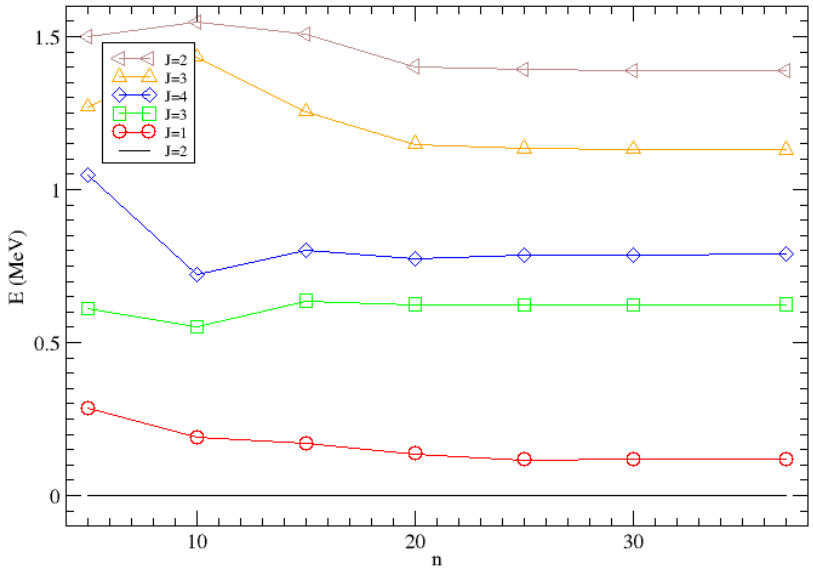

Figure 17. 28Na

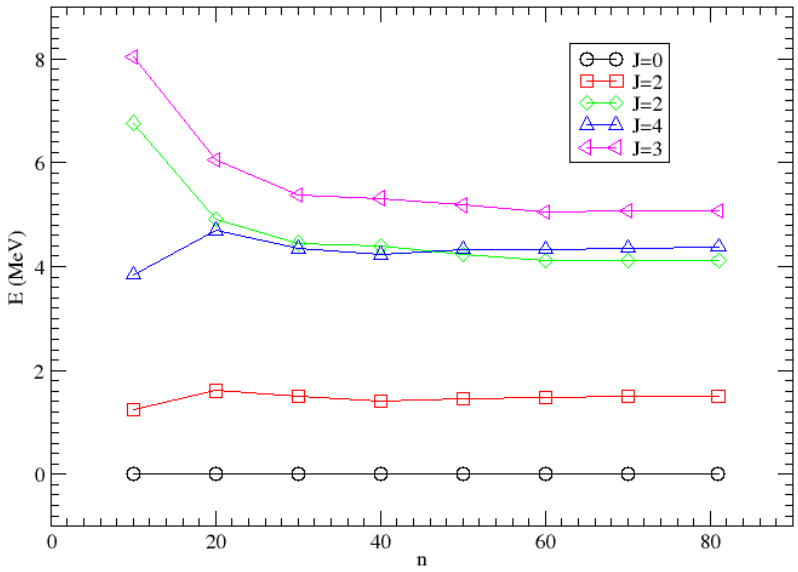

Figure 18. 24Mg

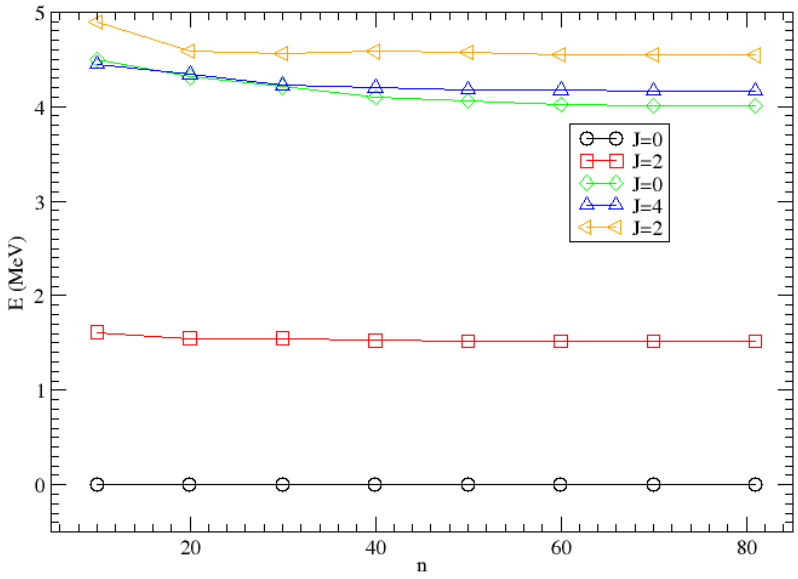

Figure 19. 28Mg

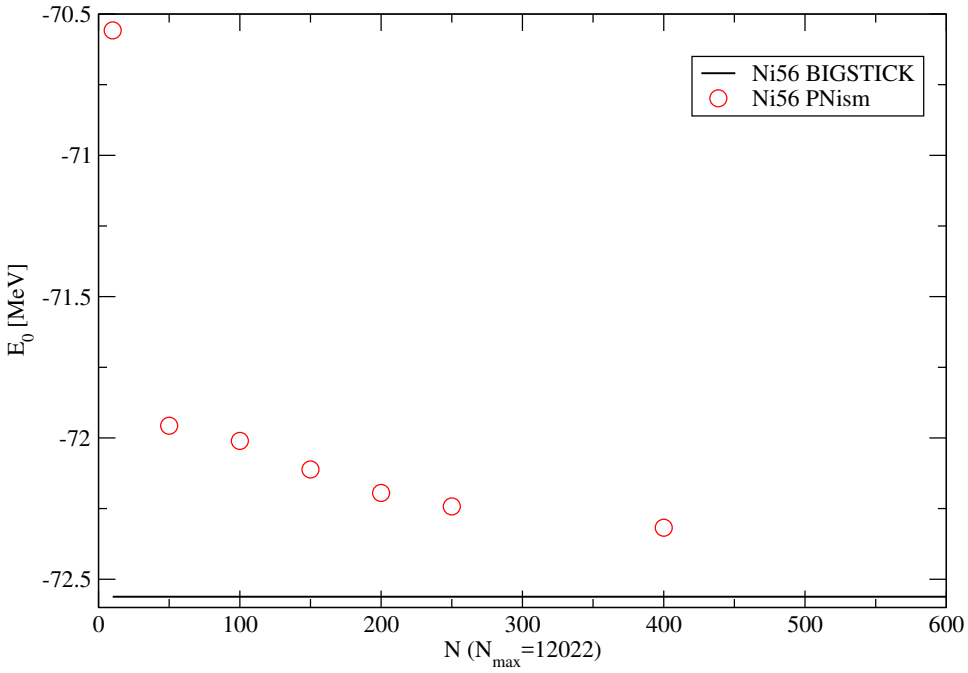

Figure 20. Ni56 Ground State Convergence

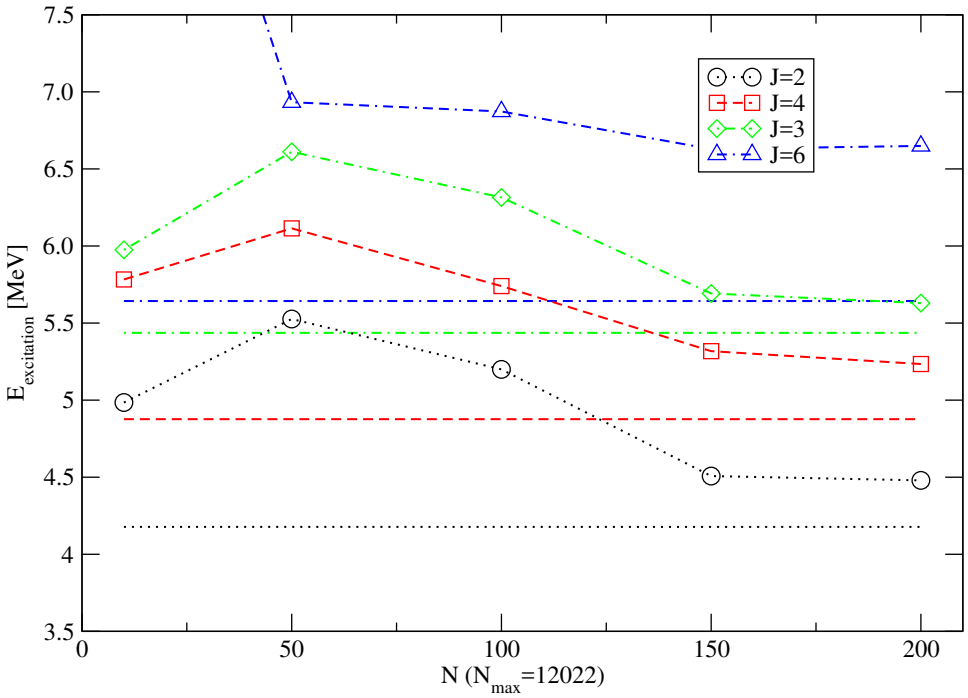

Figure 21. Ni56 Excitation Spectra

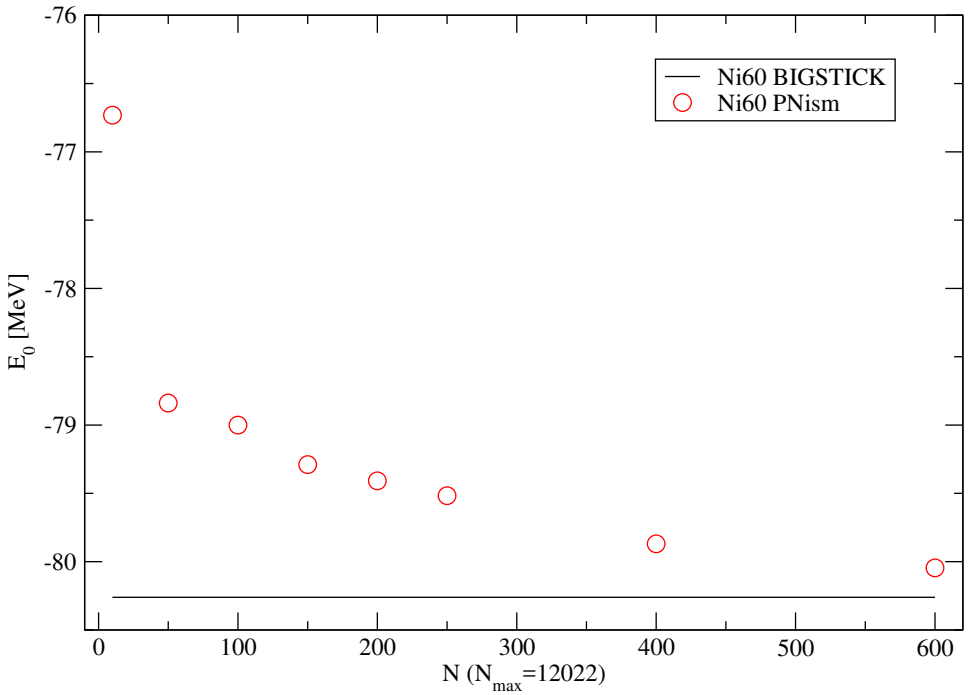

Figure 22. Ni60 Ground State Convergence

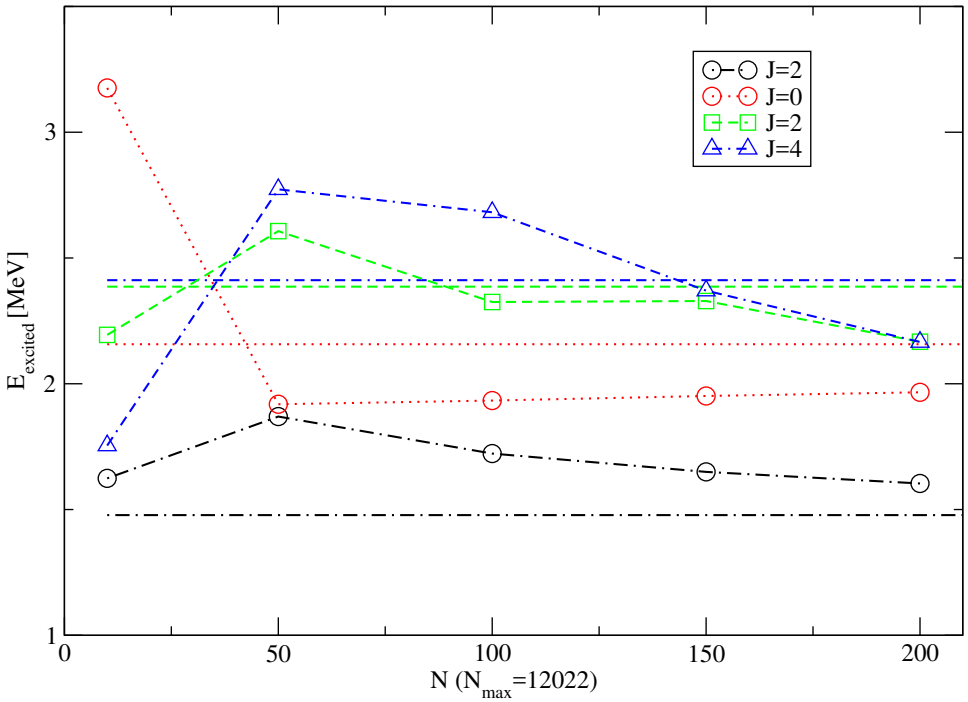

Figure 23. Ni60 Excitation Spectra

CHAPTER 7

CONCLUSION

FUTURE IMPROVEMENTS

Effective Single Particle Interactions

Order of Operations

In the current version, PNISM computes the entire set of Hamiltonian matrix elements before diagonalizing. Memory utilization could be greatly improved by diagonalizing the Hamiltonian after completing each value of total angular momentum. This is possible since PNISM is a J-scheme code; matrix elements between states with different total J are independent. Here is a pseudo-code depiction of the current procedure:

```
DO J = JMIN, JMAX
    COMPUTE <AB,J| H |CD,J>
END DO
DO J = JMIN, JMAX
    DIAGONALIZE <AB,J| H |CD,J>
END DO
DEALLOCATE <AB,J| H |CD,J>
```

The problem being that this requires storing the entire Hamiltonian in memory before diagonalizing and writing to disk the much smaller set of truncated eigenstates and quantum numbers. If instead we use the following procedure:

```
DO J = JMIN, JMAX
    COMPUTE <AB,J| H |CD,J>
    DIAGONALIZE <AB,J| H |CD,J>
    DEALLOCATE <AB,J| H |CD,J>
END DO
```

then we can expect a reduction in the total memory resources required by a factor that scales like the number of J states required. While simple in principle, this will require a nontrivial restructuring of the code.

REFERENCES

[1] C. W. Johnson, W. E. Ormand, and P. G. Krastev, "Factorization in large-scale many-body calculations," Comp. Phys. Comm. **184** (2761), 1–34 (2013).

[2] E. Epelbaum, *Nuclear forces from chiral effective field theory - a primer*, Joliot-Curie School, Lacanau, France (2009).

[3] T. C. S. E. W. Group, *Data Formats and Procedures for the Evaluated Nuclear Data File ENDF-6*, National Nuclear Data Center, Brookhaven National Laboratory (1995).

[4] N. Jeevanjee, *An Introduction to Tensors and Group Theory for Physicists* (Springer, Switzerland, 2011).

[5] A. Fetter, and J. Walecka, *Quantum Theory of Many-Particle Systems* (McGraw-Hill, New York, 1971).

[6] C. W. Johnson, W. E. Ormand, K. S. McElvain, and H. Shan, *BIGSTICK: A flexible configuration-interaction shell-model code*, Department of Physics, San Diego State University and Lawrence Livermore National Laboratory and Department of Physics, University of Californian, Berkeley and Computational Research Division, Lawrence Berkeley Laboratory (2018).

[7] P. J. Brussaard, and P. W. M. Glaudemans, *Shell-model Applications in Nuclear Spectroscopy* (North-Holland Publishing Company, Amsterdam, 1977).

[8] J. M. Eisenberg, and W. Greiner, *Microscopic Theory of the Nucleus* (North-Holland Publishing Company, Amsterdam, 1972).

[9] K. Heyde, *Basic Ideas and Concepts in Nuclear Physics* (Institute of Physics Publishing, London, 1994).

[10] T. Papenbrock, and D. J. Dean, "Factorization of shell-model ground states," Physical Review C **67** (051303), 1–5 (2003).

[11] T. Papenbrock, A. Juodagalvis, and D. J. Dean, "Solution of large scale nuclear structure problems by wave function factorization," Physical Review C **69** (024312), 1–12 (2004).

[12] T. Papenbrock, and D. J. Dean, "Density matrix renormalization group and wavefunction factorization for nuclei," J. .Phys. G: Nucl. .Part. Phys. **31** (S1377S1383), S1377S1383 (2005).

[13] A. deShalit, and H. Feshbach, *Theoretical Nuclear Physics, Volume I: Nuclear Structure* (John Wiley and Sons, INC., New York, 1974).

[14] P. Ring, and P. Schuck, *The Nuclear Many-Body Problem* (Springer-Verlag, New York, 1980).

[15] A. R. Edmonds, *Angular Momentum in Quantum Mechanics* (Princeton University Press, Princeton, NJ, 1957).

[16] R. Shankar, *Principles of Quantum Mechanics* (Springer, New York, 1994).

APPENDIX A

Supplementary Notes

Supplementary Notes

VECTOR COUPLING COEFFICIENTS

Vector coupling coefficients, commonly referred to as Clebsch Gordan Coefficients[16] are simply the coefficients of an expansion of a coupled angular momentum state with fixed total J in a basis of coupled states $|j_1 m_1, j_2 m_2\rangle \equiv |j_1 m_1\rangle \otimes |j_2 m_2\rangle$. That is to say, in the expansion

$$|j_1 j_2; JM\rangle = \sum_{m_1 m_2} |j_1 m_1, j_2 m_2\rangle \langle j_1 m_1, j_2 m_2 || j_1 j_2; JM\rangle, \tag{111}$$

the inner products $\langle j_1 m_1, j_2 m_2 || j_1 j_2; JM\rangle$ are the vector coupling coefficients. This are often written as

$$(j_1 m_1 j_2 m_2 | JM) \equiv \langle j_1 m_1, j_2 m_2 || j_1 j_2; JM\rangle \tag{112}$$

so that

$$|j_1 j_2; JM\rangle = \sum_{m_1 m_2} (j_1 m_1 j_2 m_2 | JM) |j_1 m_1, j_2 m_2\rangle. \tag{113}$$

3-J SYMBOL

A generalization of the vector-coupling coefficients are the so called three-J symbols (3-j symbols). They are defined in terms of the vector coupling coefficients for the coupling of three angular momenta:[15]

$$\begin{Bmatrix} j_1 & j_2 & j_3 \\ m_1 & m_2 & m_3 \end{Bmatrix} \equiv (-1)^{j_1 - j_2 - m_2} (2j_2 + 1)^{-1/2} (j_1 m_1 j_2 m_2 | j_1 j_2 j_3 - m - 3). \tag{114}$$

6-J SYMBOLS AND 9-J SYMBOLS

Six-J and Nine-9 symbols are further generalizations of vector coupling coefficients which often appear in calculations involving complex angular momentum algebra. Refer to Edmonds[15] for a complete description.

SINGULAR VALUE DECOMPOSITION

A singular value decomposition is a eigenvalue decomposition, generalized to non-square non-symmetric matrices. The method of singular value decomposition comes

from a theorem which tells us that any $M \times N$ matrix A with $M \geq N$ can be written as the product of an $M \times N$ column-orthogonal matrix U, an $N \times N$ diagonal matrix W with positive or zero elements (the singular values), and the transpose of an $N \times N$ orthogonal matrix V. [Numerical Recipes p51.] That is

$$A_{M\times N} = U_{M\times N} W_{N\times N} V^T_{N\times N} \tag{115}$$

or in matrix notation,

$$A_{ij} = \sum_{a=1}^{N} U_{ia} \sum_{b=1}^{N} W_{ab} V_{jb} \tag{116}$$

Which, for the case where $M = N$, simply states that we can write a matrix A as a unitary transformation of a diagonal matrix containing the eigenvalues of A:

$$A_{ij} = \sum_{ab} U_{ia} W_{ab} U_{jb}. \tag{117}$$

LANCZOS METHOD

This is a breif overview of the Lanczos method used in this research. The Lanczos Algorithm is used to obtain the extrenal eigenvalues of an $n \times n$ Hermitian matrix in $m < n$ linear operations. This is done by transforming the Hermitian matrix into a truncated tridiagonal matrix containing the extremal eigenvalues.

1. Begin with an $n \times n$ real-symmetric matrix H and a fixed number $m << n$ of iterations to carry out. Generate a random normalized vector v_0 of dimension n.

2. $For\ i = 1, ..., k$

$w = Hv_i$

$a_i = v_i w$

!Orthogonalize

$w = w - a_i v$

!Orthogonalize against prior vectors i-1

VARIATIONAL PRINCIPLE

The Variational Principle is an extremely useful theorem in quantum mehanics as it is the basis of all variational methods. The principle states that the expectation value of the Hamiltonian in any state is greater than or equal to the expectation value of the Hamiltonian in the ground state. Suppose we have a Hamiltonian $\hat{H}$ and an arbitrary state $|\phi\rangle$ both in some

Hilbert space H. Because $\hat{H}$ is Hermitian, we are guarenteed that it has a complete set of eigenvectors and eigenvalues, $|\psi\rangle_i$ and E_i. Suppose that the lowest eigenstate has some, perhaps unknown, eigenvalue E_0. The Variational Principle is that the expectation value of $\hat{H}$ in the state $|\phi\rangle$ is

$$\frac{\langle\phi|\hat{H}|\phi\rangle}{\langle\phi||\phi\rangle} \geq E_0 \tag{118}$$

This is is straightforward to prove since we can always write $|\phi\rangle = \sum_i c_i|\psi\rangle_i$. Then equation (1) can be written

$$\begin{aligned}
\frac{\langle\phi|\hat{H}|\phi\rangle}{\langle\phi||\phi\rangle} &= \frac{\sum_j c_j^*\langle\psi|_j\hat{H}\sum_i c_i|\psi\rangle_i}{\sum_j c_j^*\langle\psi|_j\sum_i c_i|\psi\rangle_i} \\
&= \frac{\sum_{j,i} c_j^* c_i\langle\psi|_j\hat{H}|\psi\rangle_i}{\sum_{j,i} c_j^* c_i\delta_{i,j}} \\
&= \frac{1}{\sum_i |c_i|^2}\sum_{j,i} c_j^* c_i E_i\delta_{j,i} \\
&= \frac{1}{\sum_i |c_i|^2}\sum_j |c_j|^2 E_j
\end{aligned} \tag{119}$$

Since $E_0 \leq E_i$ for all i, each term satisfies $|c_j|^2 E_0 \leq |c_j|^2 E_j$ and

$$\frac{1}{\sum_i |c_i|^2}\sum_j |c_j|^2 E_j \geq \frac{1}{\sum_i |c_i|^2} E_0 \sum_j |c_j|^2 \geq E_0. \tag{120}$$

This inequality allows us to propose a model wavefunction and have the guarentee that our ground state will be bounded.

APPENDIX B

Sample Density Matrix Files

Sample Density Matrix Files

Here I have provided some redacted density matrix files to provide some context for the discusison given on reading in density matrices. The following are data from input files to be read into PNISM. The format of the density matrix files is

$$\langle Final\ State|[\pi_a^\dagger \pi_c]_{J_t}|Initial\ State\rangle \tag{121}$$

These particle density matrix files are used for calculating Ne20 in the sd model space with an inert O16 core. This means that there are two valence protons and two valence neutrons. This first file contains the excitation spectra and density matrices for a nuclei with two protons and zero neutrons with $M = J_z = 0$.

```
  BIGSTICK Version 7.8.1 Sept 2017
  single-particle file = sd
           2           0    <--- #protons, #neutrons
           0 +              <--- Jz, parity
  Time to compute jumps :    9.9999993108212948E-004
  Time to compute jumps :    0.0000000000000000
  State      E        Ex         J      T
    1    -11.77906   0.00000    -0.000   1.000
    2     -9.84945   1.92961     2.000   1.000
    3     -8.37591   3.40315     4.000   1.000
...
 Initial state #    2 E =   -9.84945 2xJ, 2xT =    4   2
 Final state   #    4 E =   -7.56341 2xJ, 2xT =    4   2
 Jt =   0, proton      neutron
    1    1  -0.01892   0.00000
    2    2   0.45231   0.00000
    3    3  -0.75667   0.00000
 Jt =   2, proton      neutron
```

```
    1    1  -0.01948   0.00000
    1    2   0.04273   0.00000
    1    3  -0.00230   0.00000
    2    1  -0.05930   0.00000
    2    2  -0.65142   0.00000
    2    3   0.40773   0.00000
    3    1  -0.03520   0.00000
    3    2  -0.71134   0.00000
 Jt =   4, proton      neutron
    1    2   0.06297   0.00000
    2    1  -0.13163   0.00000
    2    2   0.08321   0.00000
...
```

This second files contains the excitation spectra and density matrices for a nuclei with two protons and zero neutrons with $M = J_z = 1$. Notice that the states number labels do not match up between the two files. The $M = J_z = 1$ results are missing states with $J = 0$; you cannot have total angular momentum less than the z-component of the angular momentum. Also notice that density matrix elements between the same states (identified by E, J, and T quantum numbers) are identical up to a phase. The $M = J_z = 1$ density matrix file also has the entire set of J_t quantum numbers for a given initial and final state while the $M = J_z = 1$ density matrix file is missing odd Jt quantum numbers. Both solutions are required by PNISM to obtain the entire density matrix.

```
  BIGSTICK Version 7.8.1 Sept 2017
  single-particle file = sd
           2           0
           2 +
  Time to compute jumps :    1.0000001639127731E-003
  Time to compute jumps :    0.0000000000000000
  State      E        Ex         J      T
    1     -9.84945   0.00000     2.000   1.000
    2     -8.37591   1.47354     4.000   1.000
```

```
    3     -7.56341   2.28605     2.000   1.000
...
Initial state #    1 E =   -9.84945 2xJ, 2xT =    4   2
 Final state   #    3 E =   -7.56341 2xJ, 2xT =    4   2
 Jt =   0, proton      neutron
    1    1   0.01892   0.00000
    2    2  -0.45231   0.00000
    3    3   0.75667   0.00000
 Jt =   1, proton      neutron
    1    1   0.01886   0.00000
    1    2  -0.03956   0.00000
    1    3   0.02182   0.00000
    2    1   0.00724   0.00000
    2    2   0.04334   0.00000
    3    1  -0.03337   0.00000
    3    3  -0.31605   0.00000
 Jt =   2, proton      neutron
    1    1   0.01948   0.00000
    1    2  -0.04273   0.00000
    1    3   0.00230   0.00000
    2    1   0.05930   0.00000
    2    2   0.65142   0.00000
    2    3  -0.40773   0.00000
    3    1   0.03520   0.00000
    3    2   0.71134   0.00000
 Jt =   3, proton      neutron
    1    1   0.02028   0.00000
    1    2  -0.03333   0.00000
    2    1   0.13226   0.00000
    2    2   0.75618   0.00000
    2    3   0.17724   0.00000
    3    2  -0.29377   0.00000
```

```
 Jt =   4, proton      neutron
    1    2  -0.06297   0.00000
    2    1   0.13163   0.00000
    2    2  -0.08321   0.00000
...
```

APPENDIX C

Additional Figures

Additional Figures

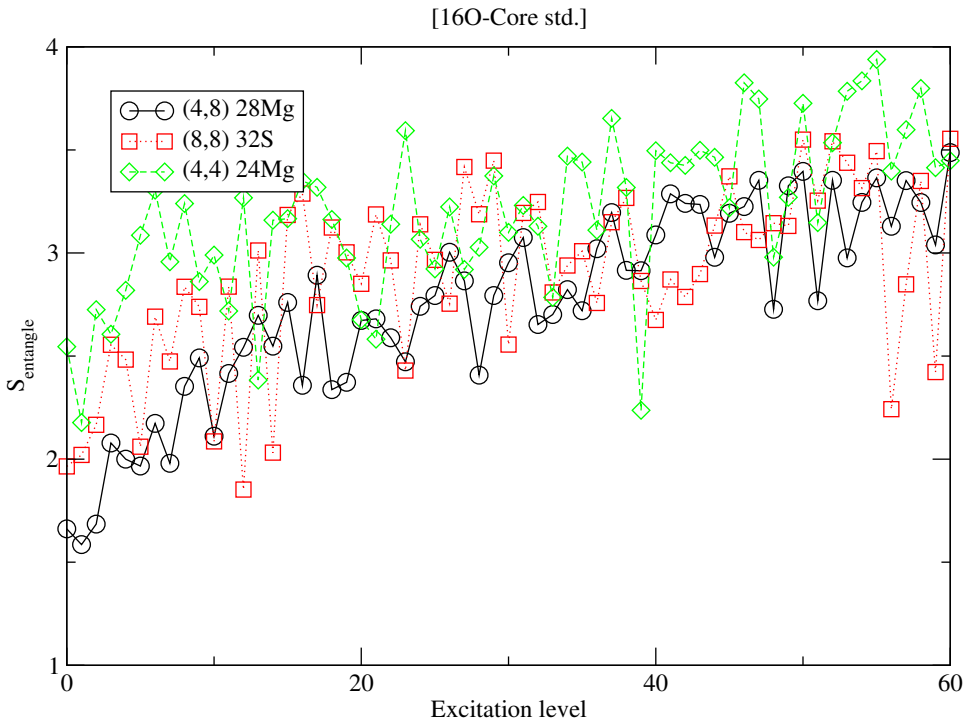

Figure 24. S vs Excitation Level: Mg

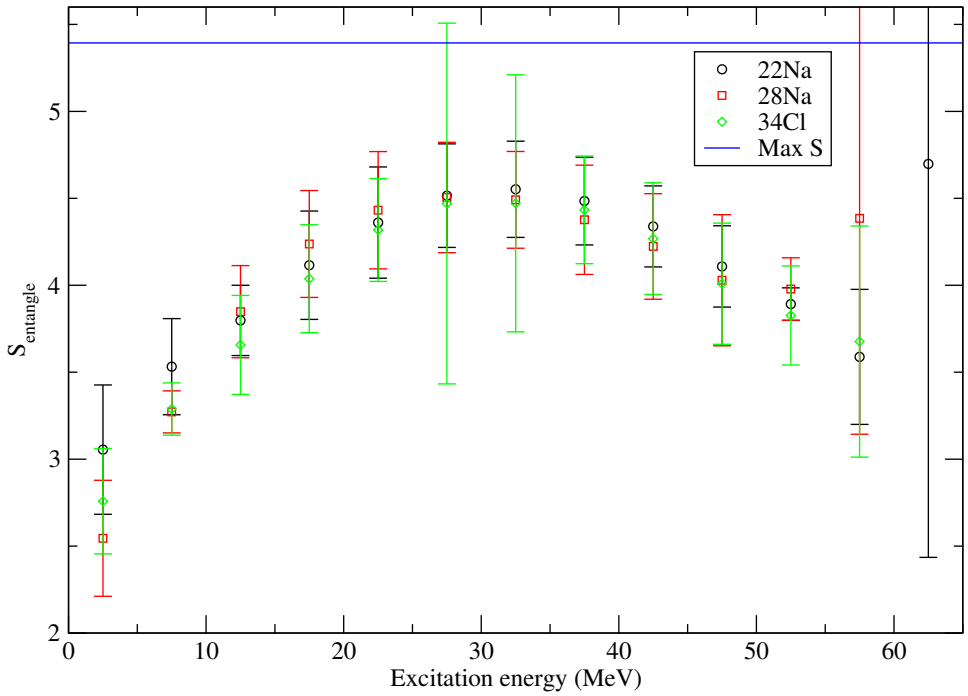

Figure 25. S vs Excitation Level: Ne

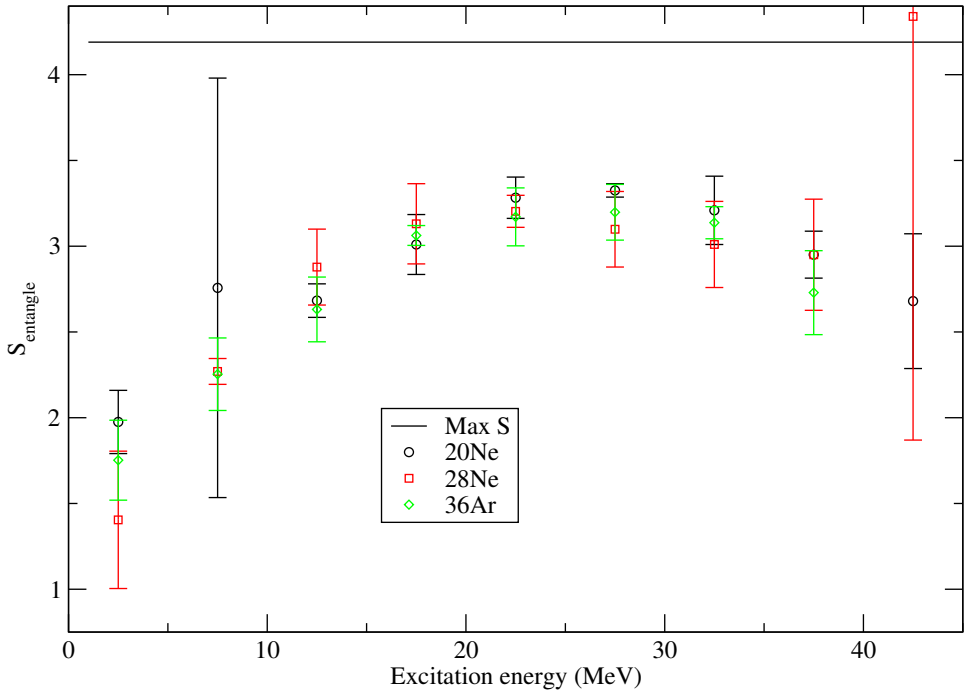

Figure 26. S vs Excitation Level: Ne

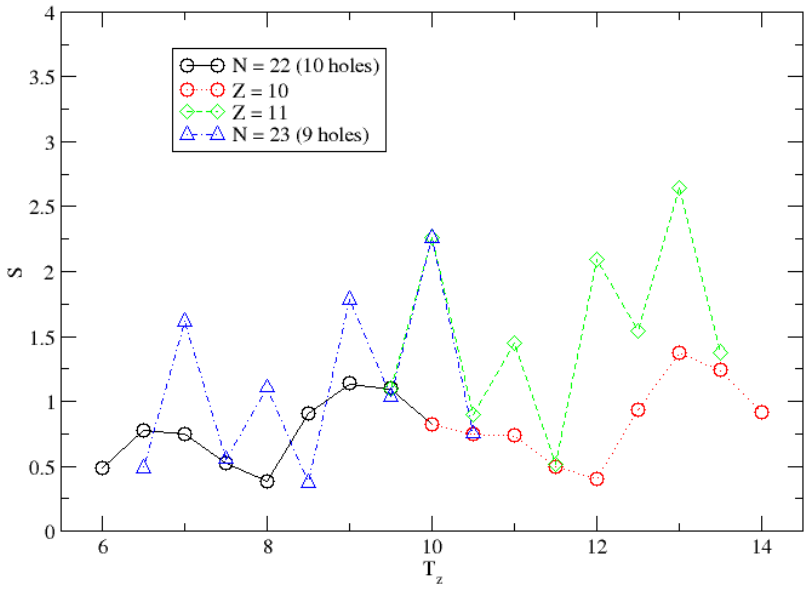

Figure 27. S vs Tz: SD-PF Shell

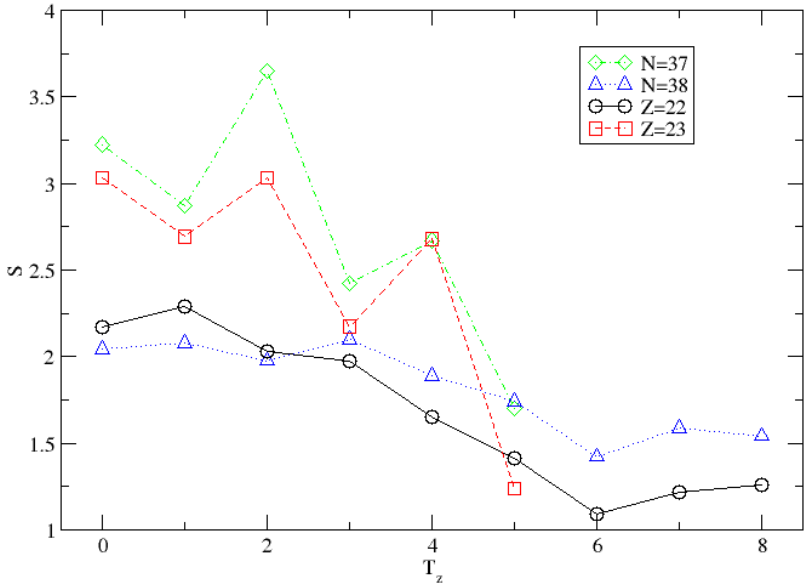

Figure 28. S vs Tz: PF Shell

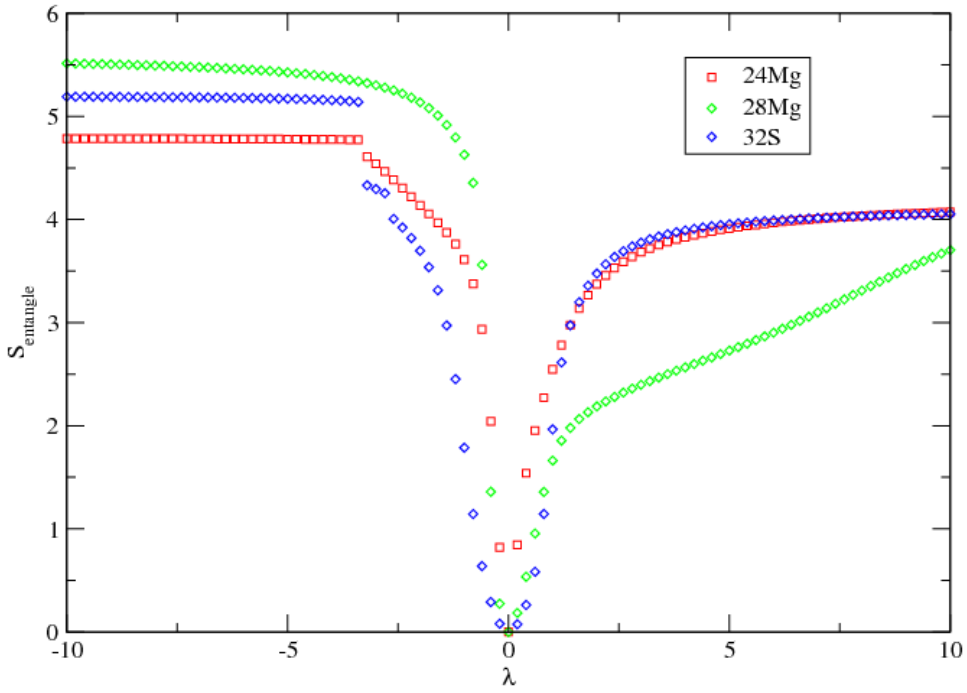

Figure 29. S vs Coupling: Mg

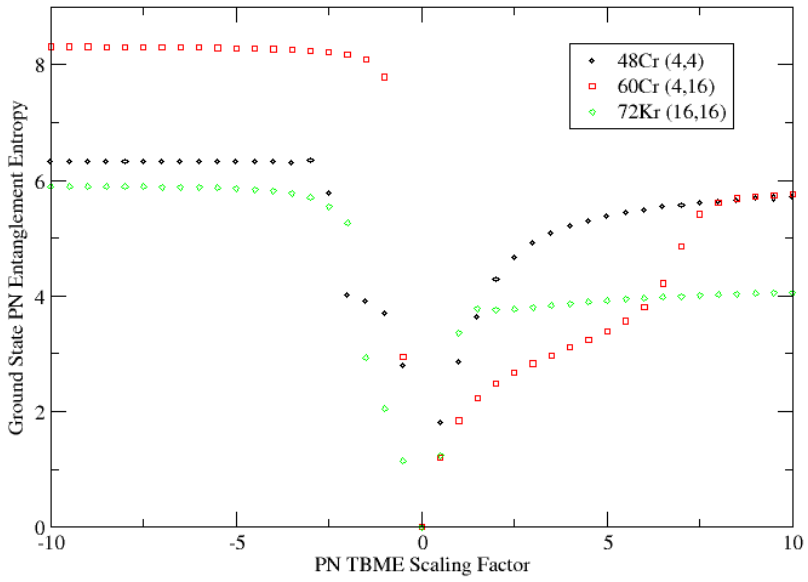

Figure 30. S vs Coupling: Cr

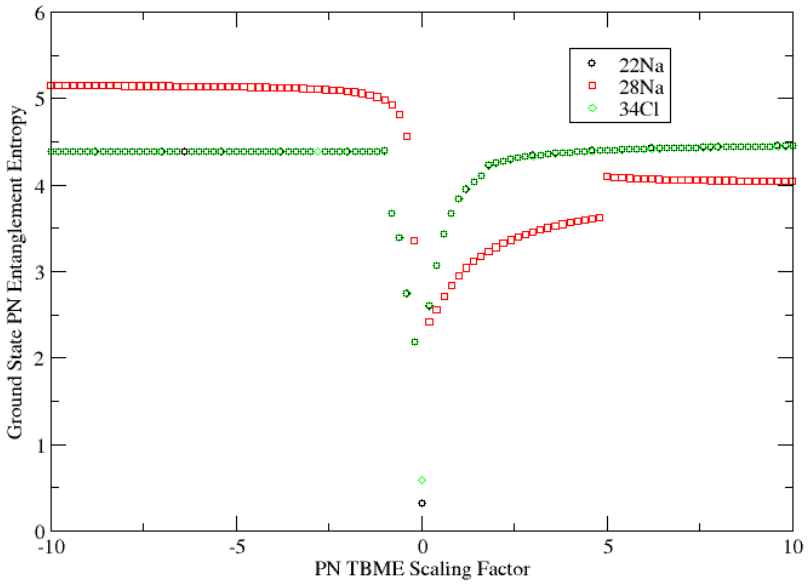

Figure 31. S vs Coupling (Traceless): Na

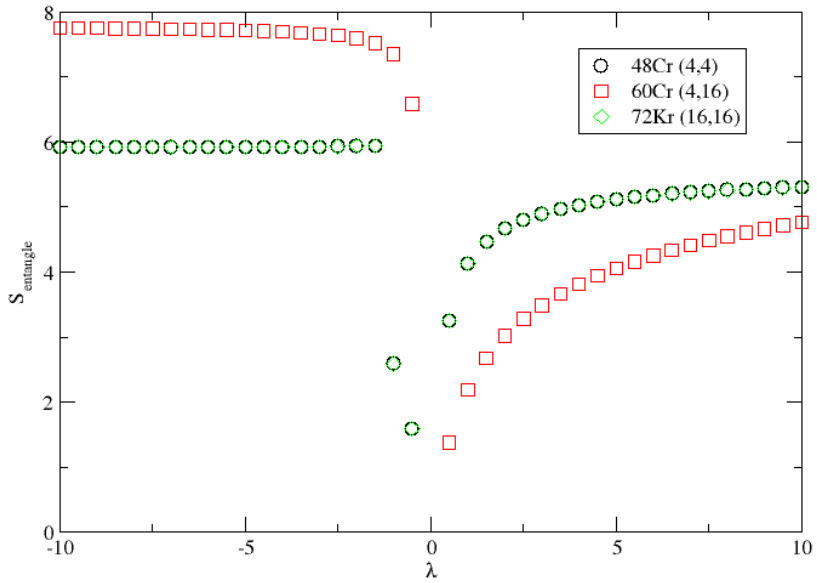

Figure 32. S vs Coupling (Traceless): Cr

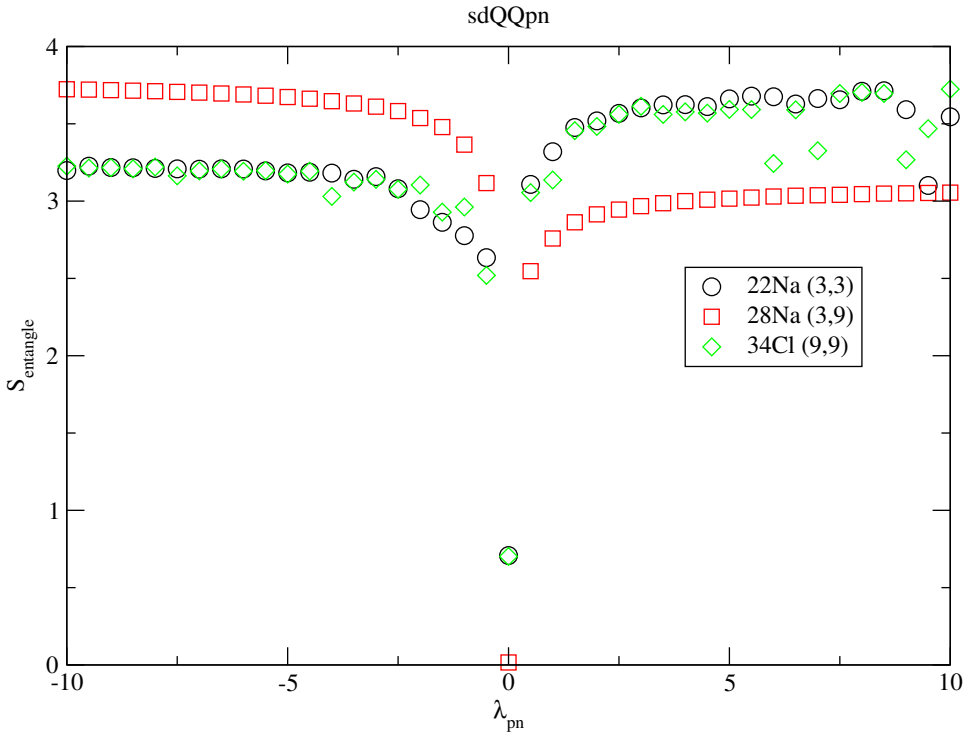

Figure 33. S vs Coupling (QQ): Na

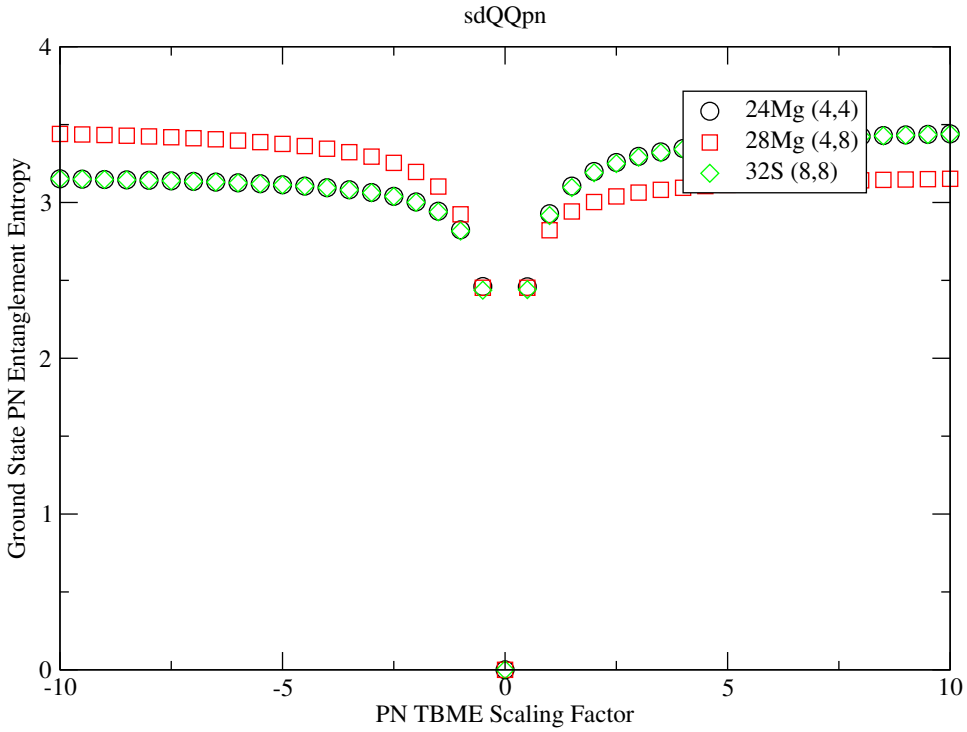

Figure 34. S vs Coupling (QQ): Mg

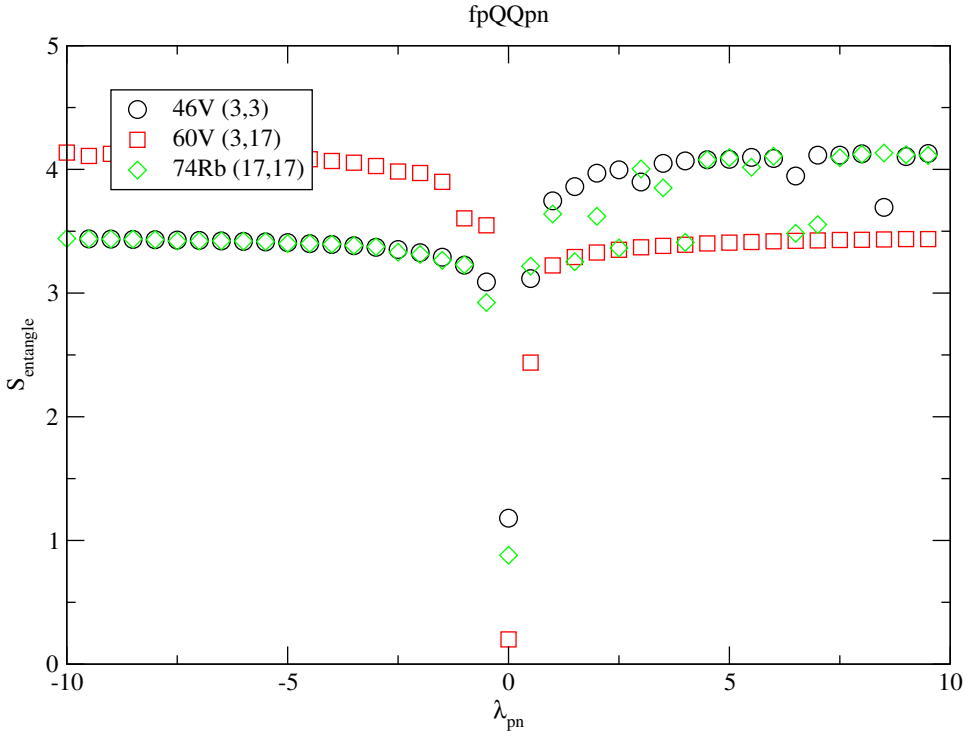

Figure 35. S vs Coupling (QQ): V

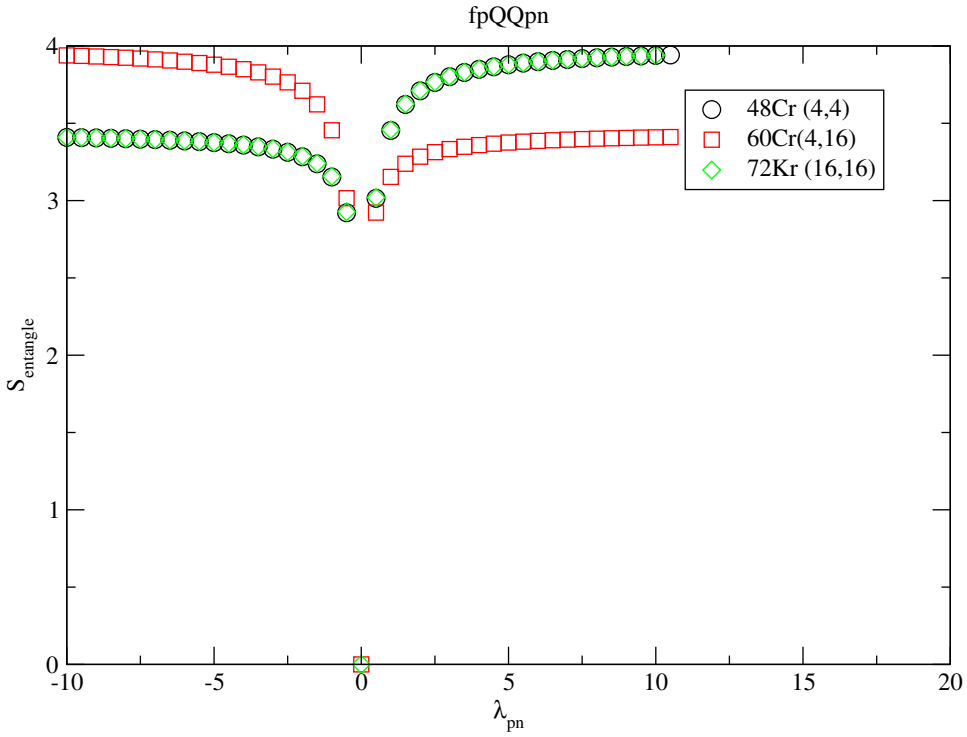

Figure 36. S vs Coupling (QQ): Cr

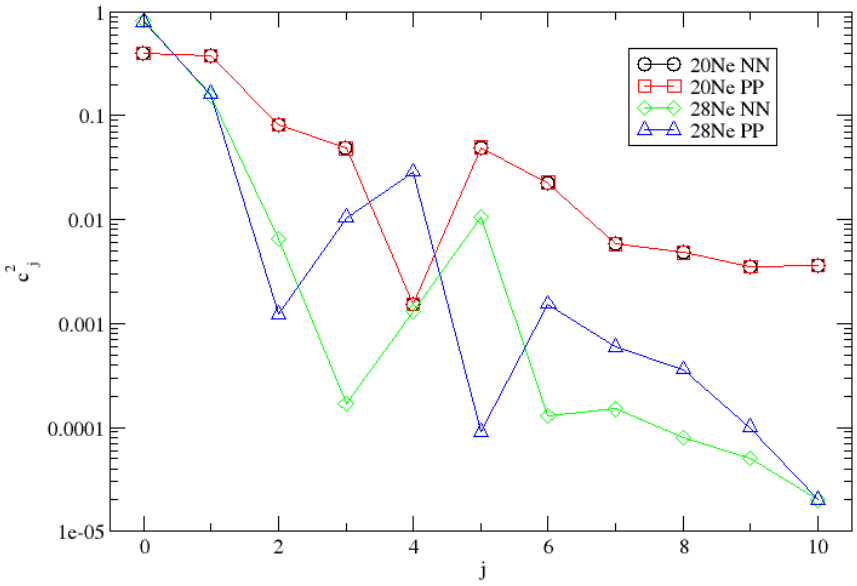

Figure 37. Proton-Neutron Decomposition: Ne and PH-Conjugates

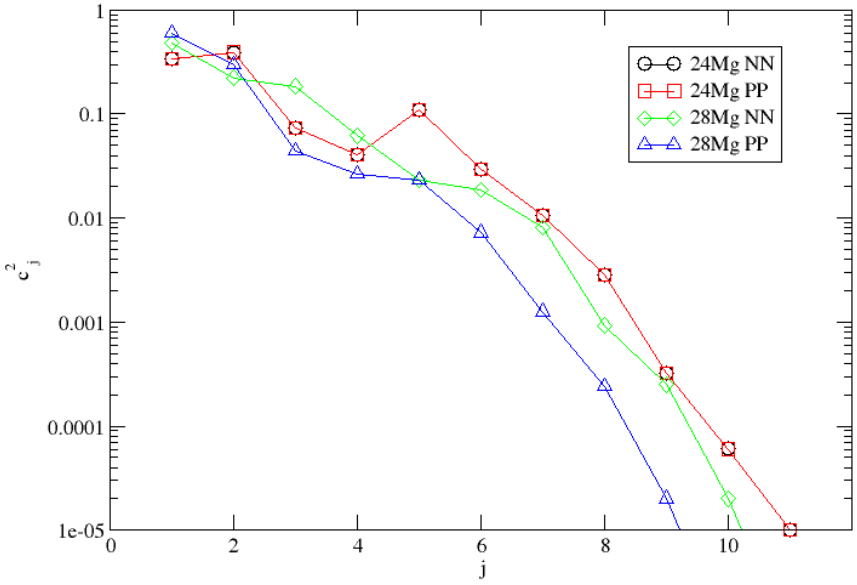

Figure 38. Proton-Neutron Decomposition: Mg and PH-Conjugates

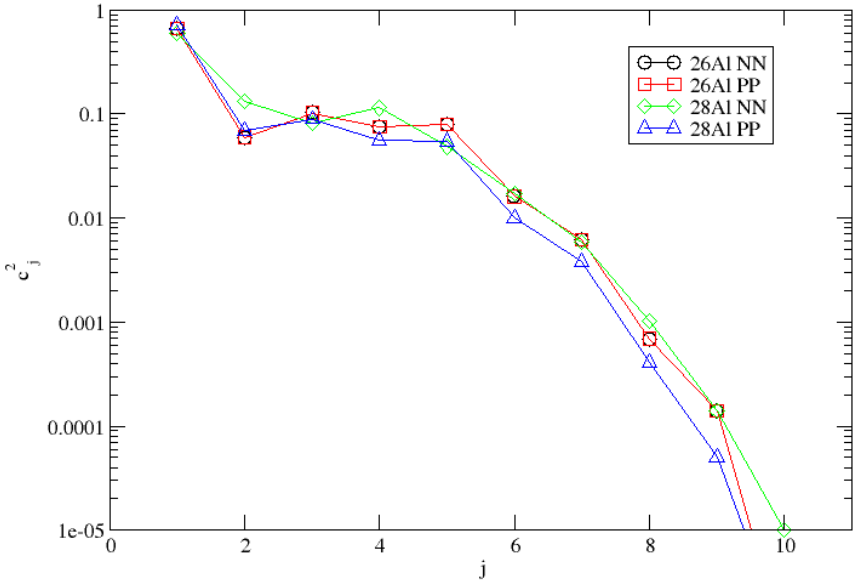

Figure 39. Proton-Neutron Decomposition: Al and PH-Conjugates

ABSTRACT OF THE THESIS

Efficient Calculation of Nuclear Wavefunctions
Through Coupling of Proton
and Neutron Wavefunctions
by
Oliver Gorton
Master of Science in Physics
San Diego State University, 2018

This thesis describes a nuclear shell model code which allows for a significant reduction in computer resource usage while retaining accuracy of results as compared to numerically exact solutions. I begin with an introduction to configuration interaction nuclear physics and shell model calculations. I then motivate the need for a proton-neutron decomposition of the Hamiltonian and present evidence for the viability of such a decomposition to reduce the size of the model space through three different studies. The first is a series of calculations of proton-neutron entanglement entropy, a relatively novel approach in shell model calculations. Entanglement entropy measures the distribution of singular value decomposition eigenvalues, and thus the viability of truncation of a model space. These calculations involve studying the strength and origin of the isospin dependence of the proton-neutron entanglement entropy. The second is a toy model that attempts to reproduce the entanglement entropy properties seen in realistic nuclear calculations. The third is a strength function decomposition of exact wavefunctions in an explicit proton-neutron formalism. Finally, I discuss a code to calculate nuclear wave-functions by a coupling of proton and neutron wave-functions which are calculated beforehand by an existing interacting shell model code. Results and convergence properties of this code are provided and discussed.